



TRIBHUVAN UNIVERSITY
INSTITUTE OF ENGINEERING
PULCHOWK CAMPUS

THESIS NO: M-72-MSMDE-2021-2023

TEMPERATURE ANALYSIS OF ELECTRIC VEHICLE LITHIUM ION CELL

by:

ANUSKA GAUTAM

A THESIS
SUBMITTED TO THE DEPARTMENT OF MECHANICAL AND AEROSPACE
ENGINEERING IN PARTIAL FULFILLMENT OF THE REQUIREMENTS
FOR THE DEGREE OF MASTER OF SCIENCE IN
MECHANICAL SYSTEMS DESIGN AND ENGINEERING

DEPARTMENT OF MECHANICAL AND AEROSPACE ENGINEERING
LALITPUR, NEPAL

NOVEMBER, 2023

COPYRIGHT

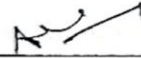
The author has agreed that the library, Department of Mechanical and Aerospace Engineering, Pulchowk Campus, Institute of Engineering may make this thesis freely available for inspection. Moreover, the author has agreed that permission for extensive copying of this thesis for scholarly purpose may be granted by the professor(s) who supervised the work recorded herein or, in their absence, by the Head of the Department wherein the thesis was done. It is understood that the recognition will be given to the author of this thesis and to the Department of Mechanical and Aerospace Engineering, Pulchowk Campus, Institute of Engineering in any use of the material of the thesis. Copying or publication or the other use of this thesis for financial gain without approval of the Department of Mechanical and Aerospace Engineering, Pulchowk Campus, Institute of Engineering and author's written permission is prohibited.

Request for permission to copy or to make any other use of the material in this thesis in whole or in part should be addressed to:

Head Department of Mechanical and Aerospace Engineering
Pulchowk Campus,
Institute of Engineering
Lalitpur, Nepal

**TRIBHUVAN UNIVERSITY
INSTITUTE OF ENGINEERING
PULCHOWK CAMPUS
DEPARTMENT OF MECHANICAL AND AEROSPACE ENGINEERING**

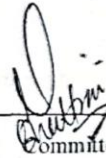
The undersigned certify that they have read, and recommended to the Institute of Engineering for acceptance, a thesis entitled "**Temperature Analysis of Electric Vehicle Lithium Ion Cell**" submitted by Anuska Gautam in partial fulfillment of the requirements for the degree of Masters of Science in Mechanical Systems Design and Engineering.



Associate Professor Dr. Ajay Kumar Jha,
Supervisor
Department of Mechanical and Aerospace Engineering



Er. Sagar Mani Gnawali,
External Examiner,
Nepal Electricity Authority



Committee Chairperson,
Asst. Professor Dr. Sudip Bhattrai
Head of the Department,
Department of Mechanical and Aerospace Engineering

Date: 11/27/2023

ABSTRACT

A lot of research has been done for constant discharge process of lithium-ion batteries, but study on thermal behavior of lithium-ion batteries during operation under realistic cycles is scarce. So, the main aim of this study was to better understand the temperature variation of a lithium-ion battery cell when it is charging/discharging.

For this study, the thermal responses of a lithium ion cell will be carried out in ANSYS and compared. To accomplish this, each cell was be subjected to several discharge and charging processes. The result obtained was in form of temperature contours and plots evaluating which the thermal response of the cell was compared. In ANSYS, first a cell was simulated with a series of simple discharges at various C-rates. Next, a combined cycle with few alternating charge/discharge processes will be prepared, and the changes in the temperature, total heat and voltage will be observed.

The simulations were done for various constant discharge rates. An evaluation of the result from discharge according to discharge rates ranging of 0.3 C, 1C and 3 C for environmental temperature of 300K was done. Then the cells and module were simulated by employing different cooling fluids. The change in maximum temperature was observed and the appropriate coolant was selected. A sample test to observe the temperature increase in cell during discharging was performed for 0.3 C and its results were noted. For simple discharge, 3M Novec 7100 is found to be a better cooling fluid. While for charge discharge cycles, water was found to be better coolant.

Keywords: Lithium ion cell, ANSYS, NTGK module, temperature, charge/discharge cycle, discharge rate, C-rate

ACKNOWLEDGEMENTS

I extend my deepest gratitude to my supervisor Associate Professor Dr. Ajay Kr. Jha for his unwavering guidance and supervision throughout the entirety of my thesis work. His expertise and support were instrumental in bringing this project to fruition, and without his valuable insights, this endeavor would not have reached its completion.

The faculty of Mechanical and Aerospace Engineering at Pulchowk Campus has played an indispensable role in shaping the trajectory of this work. Their consistent advice, valuable suggestions, and profound insights provided a solid foundation from the inception to the conclusion of this project. I am truly thankful for their unwavering support.

Special appreciation goes to the National Innovation Centre in Kirtipur for generously providing the necessary space for conducting crucial tests on the battery. The assistance from this center significantly contributed to the successful execution of the research. I express my sincere thanks to Er. Shyam Kr. Thakur and Er. Najam Rain, whose guidance and efforts were pivotal in making this aspect of the project possible.

The support from my friends at MSMDE Pulchowk has been a constant pillar throughout this journey. Their encouragement and assistance have been invaluable, and I extend my thanks to each one of them for their contributions. I would also like to thank Er. Bibek Dhakal, Er. Udip Prajapati and Er. Suraksha Pal who have always backed this work and encouraged me to complete it.

Last but not least, I owe a debt of gratitude to my family. Their unwavering support, patience, and encouragement were the bedrock upon which I built this thesis. Without them, this achievement would not have been possible. I am truly blessed to have such a supportive foundation that has played a crucial role in this academic milestone.

TABLE OF CONTENTS

COPYRIGHT	ii
ABSTRACT.....	iii
ACKNOWLEDGEMENTS.....	v
TABLE OF CONTENTS	vi
LIST OF TABLES.....	ix
LIST OF FIGURES.....	x
LIST OF ACRONYMS AND ABBREVIATIONS.....	xiii
CHAPTER ONE: INTRODUCTION.....	1
1.1 Introduction to Electric Vehicle.....	1
1.2 Lithium-ion battery	2
1.3 Battery Thermal Management System.....	3
1.4 Drive Cycle:.....	4
1.5 Does drive cycle affect temperature?.....	5
1.6 Thermal runaway:	6
1.7 Problem Definition and aim:	6
1.8 Objectives:	7
1.8.1 Main Objective:	7
1.8.2 Specific Objectives:.....	7
1.9 Limitations of the Study:.....	7
CHAPTER TWO: LITERATURE REVIEW	8
2.1 EV Challenges and Opportunities in Nepal	11
2.2 Introduction to C-rate.....	12
2.3 Types of Battery Configuration used in Electric Vehicles:.....	13

2.4 Coolants.....	15
CHAPTER THREE: RESEARCH METHODOLOGY	17
3.1 Literature Review:	17
3.2 Conceptual Framework:	18
3.3 Experimental Setup.....	19
3.4 Analytical Design of the cell	19
3.4.1 For LG Chem cell:	19
3.4.2 For Highstar cell:	20
3.5 Mesh.....	20
3.6 Numerical Simulation	22
3.6.1 Models of Battery Simulation in ANSYS	22
3.6.2 Approaches of Simulation:	23
3.6.3 Setup.....	25
3.6 Result interpretation, conclusion and documentation	30
CHAPTER FOUR: RESULTS AND DISCUSSION.....	31
4.1 For Single Cell (LG Chem):	31
4.2 For battery pack (LG Chem)	46
4.3 For battery pack running on charge/discharge cycle:	54
4.4 For Highstar Cell :.....	59
4.5 Experimental Works:	67
CHAPTER FIVE: CONCLUSION AND RECOMMENDATIONS	73
5.1 Conclusion.....	73
5.2 Recommendations:.....	73
Appendix:.....	74

REFERENCES76

LIST OF TABLES

Table 1 Battery configuration information of some Electric Vehicles (400-800 V) (evkx, n.d.).....	14
Table 2 The temperature variation for single cell with different coolants and discharge rates	38
Table 3 Maximum temperature variation for single cell cooled with various coolants	45
Table 4 Temperature variation for battery pack under different discharge cycle and coolants	53
Table 5 Temperature variation for battery pack with and without coolants	59
Table 6 Table for comparison of cooling for highstar cell	63
Table 7 Temperature comparison for highstar cell under charge discharge cycle with different coolants	67
Table 8 Temperature values obtained from tests	70
Table 9 Experimental data and simulation.....	75

LIST OF FIGURES

Figure 1 Different types of Batteries (Deng, 2015).....	3
Figure 2 Different types of BTMS (Fayaz, et al., 2022).....	4
Figure 3 Conceptual Framework.....	18
Figure 4 Geometry of single cell and 3s1p battery pack	20
Figure 5 Highstar cell	20
Figure 6 Meshed structures.....	21
Figure 7 Meshed structure of highstar cell	21
Figure 8 default parameter for NTGK.....	26
Figure 9 setting for different solution options	28
Figure 10 Charge/ discharge combination file in .txt	28
Figure 11 thermal conditions	29
Figure 12 Boundary condition at inlet.....	29
Figure 13 Pressure specification at outlet.....	30
Figure 14 Contours of temperature at 0.3C, 1C and 3C respectively.....	31
Figure 15 Potential contours at 0.3 C, 1C and 3C.....	32
Figure 16 Maximum cell temperature variation for 0.3C, 1 C and 3C.....	33
Figure 17 Phi+ plots across the different C-rates.....	33
Figure 18 Contours of Temperature at 0.3 C, 1C and 3C respectively	34
Figure 19 Contours for temperature for c-rate 0.3	35
Figure 20 Contour for potential.....	35
Figure 21 Temperature contour of cell at 1 C.....	35
Figure 22 Plots for temperature and temperature contour of water-cooled cell at 3C	36
Figure 23 Temperature contour and maximum temperature plots of 3M Novec cooled cell at 0.3 C.....	36
Figure 24 Temperature contour and potential contours of water cooled cell at 1 C.....	37
Figure 25 Temperature contour of temperature at 3C for water cooled cell	37
Figure 26 Plots of Maximum temperature, Minimum temperature, and potential for single cell- under charge/discharge cycle	40

Figure 27 Plots of Maximum temperature, Minimum temperature, and potential for single cell- under c/d cycle (air cooled)	42
Figure 28 Contours for temperature and potential across the cell.....	42
Figure 29 contours for potential and static temperature of water cooled cell.....	43
Figure 30 Plots for maximum temperature and total heat generation	43
Figure 31 Contours for ϕ^+ and static temperature of 3M novec 7100 cooled cell under cycle.....	44
Figure 32 Plots for Total heat generation and Maximum temperature.....	44
Figure 33 Maximum temperature across the charge discharge cycle with and without coolants	45
Figure 34 Temperature contour at 0.3 C.....	46
Figure 35 Plot for maximum temperature at 1C	46
Figure 36 Temperature plot, Temperature and potential contours for 3C discharge rate of battery pack.....	47
Figure 37 Temperature contour of the battery pack at 0.3 C rate	48
Figure 38 Maximum temperature and Temperature contour of battery pack at 1C.....	48
Figure 39 Maximum temperature and Temperature contour of battery pack at 3C.....	49
Figure 40 Temperature contour of water cooled system at 0.3 C	50
Figure 41 Temperature contour of water-cooled system at 1 C and 3C.....	50
Figure 42 Maximum temperature of battery pack cooled by 3M Novec under discharge 51	
Figure 43 Temperature contour for 3-M Novec cooled pack at 0.3 C	51
Figure 44 Temperature contour for 3-M Novec cooled pack at 1C and 3C respectively ..	52
Figure 45 Variation of maximum temperature of pack across charge/discharge cycle	54
Figure 46 Temperature variation for battery pack under charge/discharge cycle.....	54
Figure 47 Plots for temperature, ϕ and temperature contour for air-cooled battery pack	55
Figure 48 Potential contour of cell	56
Figure 49 Maximum temperature across the drive cycle.....	56
Figure 50 Temperature contour of water-cooled battery pack under c/d cycle	57

Figure 51 Maximum temperature plot and temperature contour for water cooled battery pack.....	58
Figure 52 Maximum temperature vs flow time plots for battery pack with and without coolants	58
Figure 53 Temperature contour of cells at 0.3 C, 1C and 3C	60
Figure 54 Temperature contour of air-cooled cells at 0.3, 1 and 3C.....	61
Figure 55 Temperature of cell with and without cooling fluid(water) at 0.3 C	61
Figure 56 Temperature contour of cell cooled at 1C and 3C.....	62
Figure 57 Temperature contours of cell cooled by 3M Novec 7100 at 0.3C, 1C and 3C .	63
Figure 58 Temperature Contour, Maximum temperature, minimum temperaure and positive potential plots	65
Figure 59 Temperature contour of cell cooled by air and water	66
Figure 60 Temperature contour of cell cooled by 3M Novec 7100	66
Figure 61 Comparison of temperature with and without coolants	66
Figure 62 Setup for conducting tests	68
Figure 63 Voltage current plots for cell at 0.3C.....	69
Figure 64 Phi+ plot from simulation at 0.3 C	70
Figure 65 Experimental and simulation data for highstar cell at 0.3 C	71
Figure 66 Temperature contour for simulation at 0.3C	72
Figure 67 Experimental cell	74
Figure 68 Infrared contactless thermometer	74
Figure 67 Experimental cell	Error! Bookmark not defined.
Figure 68 Infrared contactless thermometer	Error! Bookmark not defined.

LIST OF ACRONYMS AND ABBREVIATIONS

EV	Electric Vehicle
BTMS	Battery Thermal Management System
LIB	Lithium Ion Battery
HEV	Hybrid Electric Vehicle
PHEV	Plug in Hybrid Electric Vehicle
NEA	Nepal Electricity Authority
SOC	State of Charge
DOD	Depth of Discharge

CHAPTER ONE: INTRODUCTION

1.1 Introduction to Electric Vehicle

Electric vehicles (EVs) are a type of vehicle that is powered by one or more electric motors. EVs use electricity stored in rechargeable batteries as their primary source of power, rather than relying on gasoline or diesel fuel. The batteries can be charged by plugging the automobile into an external power supply, such as a charging station, or by using an on-board generator that converts other forms of energy (such as gasoline or hydrogen) into electricity.

There are several types of EVs available, including:

1. **Battery Electric Vehicles (BEVs):** These are fully electric vehicles that rely solely on electricity from batteries to power the vehicle. They do not have an IC engine, and so emit no tailpipe emissions.
2. **Plug-In Hybrid Electric Vehicles (PHEVs):** They have both an internal combustion engine and an electric motor. They can run on electricity from the battery, gasoline from the engine, or a combination of both. PHEVs are typically able to travel longer distances than BEVs on a single charge, but still emit tailpipe emissions when running on gasoline.
3. **Hybrid Electric Vehicles (HEVs):** HEVs also have both an electric motor and an internal combustion engine, however the battery stays smaller than that of a PHEV and can only be recharged by the engine and regenerative braking. HEVs are more fuel-efficient than traditional gasoline-powered vehicles, but still emit tailpipe emissions.

Benefits of EVs include lower fuel costs, lower greenhouse gas emissions, and better air quality. However, there are also some challenges associated with EVs, such as limited driving range and a need for more charging infrastructure.

1.2 Lithium-ion battery

Because of its high voltage, high energy density, and low self-discharge rate, the lithium-ion battery (LIB) is a favored power source for hybrid electric vehicles (HEVs) and electric cars (EVs). The following properties of these batteries have made them suitable both for automotive and stationary applications.

Lithium-ion batteries are used in electric vehicles (EVs) for several reasons:

1. **High energy density:** These batteries have a higher energy density than other batteries, which means they can store extra energy in a smaller and lighter package. This is important for EVs, which require a large amount of energy to power the vehicle and need to keep the weight of the battery as low as possible.
2. **Fast charging:** They can be charged swiftly, which is important for EVs that need to be recharged swiftly during long trips or at public charging stations.
3. **Long life:** These batteries have a long lifecycle compared to other types of batteries, which is important for EVs that are designed to last for many years.
4. **Low maintenance:** These batteries require very little maintenance, which is important for EV owners who want a low-maintenance vehicle.
5. **Environmentally friendly:** Lithium-ion batteries are more environmentally friendly than other types of batteries because they do not contain lethal metals such as cadmium or lead.

Overall, the usage of Li-ion batteries in EVs allows for a more efficient and practical electric vehicle that can compete with traditional gasoline-powered vehicles in terms of range, performance, and convenience.

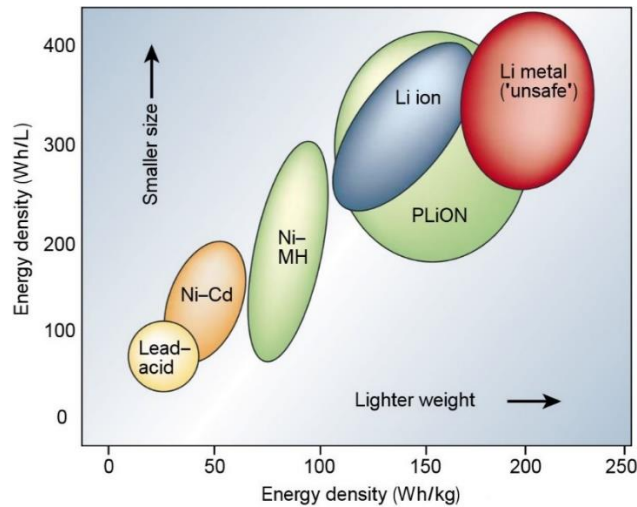


Figure 1 Different types of Batteries (Deng, 2015)

Yet despite its appealing prospects, Li-ion battery-powered EVs have not been generally welcomed by the market. This might be due to its expense, temperature-related issues, safety problems, and limited lifecycle. (Conte, 2006).

The temperature of the battery affects not just its performance but in the long run also affects the safety, and lifecycle of the battery. Researchers have shown that the optimum operating range of the battery is 15-35°C after which the lifespan and performance will deteriorate. This might lead to hazardous incidents like thermal runaway. Not just the temperature of a cell, but the temperature difference among the cells in the module should also be controlled, or else it will affect its operation and aging.

1.3 Battery Thermal Management System

Battery thermal management systems (BTMS) are designed to regulate the temperature of lithium-ion batteries in electric vehicles (EVs) and other applications. A BTMS is typically made up of several components, including a thermal management controller, sensors, and cooling or heating elements. The thermal management controller monitors the temperature and controls the operation of the cooling or heating elements to maintain the battery within the desired temperature range. The sensors provide feedback to the controller about the battery temperature and other factors, such as rate of battery discharge and the ambient temperature.

BTMS use several thermal management techniques and coolants, such as liquid cooling, air-cooling and phase change materials (PCM) (Kim, Oh, & Lee, 2019).

Liquid coolants are generally deemed more efficient than the other two options, due to their higher thermal conductivity than air and PCM.

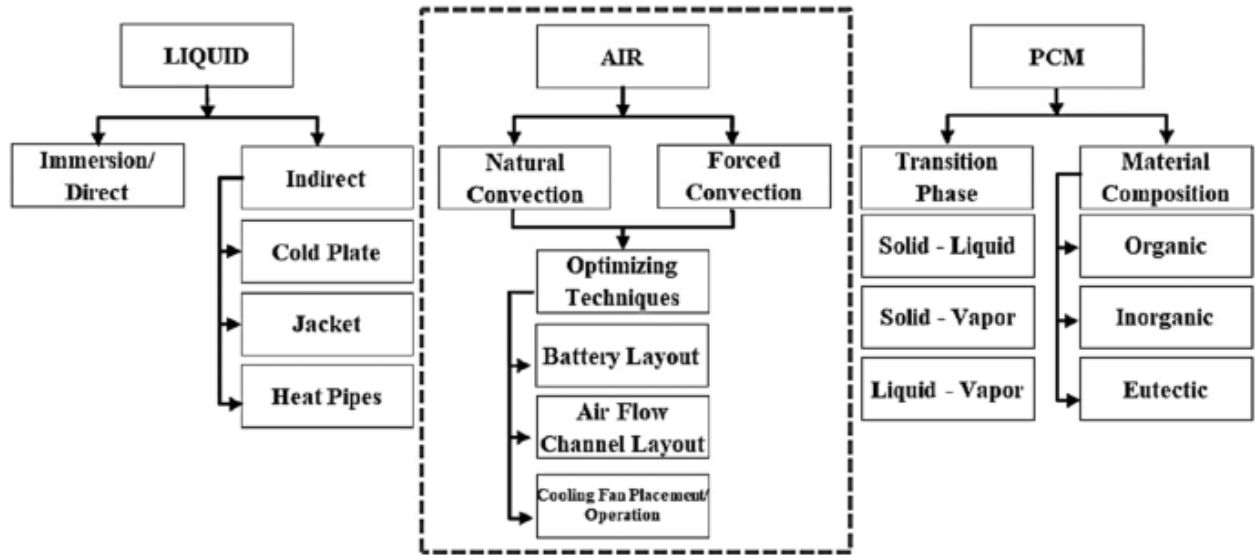


Figure 2 Different types of BTMS (Fayaz, et al., 2022)

The use of a BTMS is essential for confirming the safety and performance of lithium-ion batteries in EVs and other applications. It allows for efficient and effective regulation of the battery temperature, extending the lifespan of the battery and improving its overall performance.

The BTMS is critical in EV applications because the precision of battery management algorithms has a major influence on battery life and performance. As a result, developing a credible model to forecast the temperature dependency of LIB performance is critical to enhance battery management algorithms.

1.4 Drive Cycle:

A drive cycle is a set of driving conditions that are defined by a specific sequence of speeds and durations, which are designed to simulate real-world driving conditions. A driving

cycle is a set of data points that show a vehicle's speed over time. Many institutions and governments have devised driving cycles to evaluate automotive performance in areas such as fuel efficiency, hazardous pollutants and electric vehicle autonomy. (Bharathwaaj, et al., 2022).

The speed vs. time profile of a drive cycle typically includes information about the range of speeds that a vehicle should reach, as well as the duration of each driving event. For example, a drive cycle might include periods of steady-state cruising at highway speeds, as well as periods of stop-and-go driving in urban areas.

Drive cycles are used in many different contexts, including in the testing and evaluation of electric vehicles (EVs). By simulating real-world driving conditions, drive cycles provide a standardized way to evaluate the performance and efficiency of different EV models, and to compare them against one another.

1.5 Does drive cycle affect temperature?

The drive cycle can have a momentous impact on the temperature of the battery in electric vehicles (EVs). This is because the battery is subject to a range of different loads and operating conditions during different driving scenarios, which can cause the temperature of the battery to vary.

For example, during urban driving conditions that involve frequent stop-and-go driving, the battery may be subject to more frequent charge and discharge cycles, which can produce excess heat and can cause its temperature to increase. On the other hand, during steady-state cruising at highway speeds, the battery may be subject to less frequent charge and discharge cycles, which can result in less heat generation and lower temperatures.

In addition, the speed and acceleration profile of the drive cycle can also have an impact on the temperature of the battery. Rapid acceleration or deceleration can generate more heat than gradual changes in speed, and high speeds can also increase the temperature of the battery due to elevated wind resistance and higher current demands.

So, the drive cycle is an important factor to consider when designing a battery thermal management system for EVs. By understanding the specific driving conditions that a vehicle is likely to encounter, designers can optimize the thermal management system to

provide effective cooling or heating as needed, and to maintain safe operating temperatures for the battery.

1.6 Thermal runaway:

Thermal runaway is a phenomenon that can occur in lithium-ion batteries (LIBs) when the battery cells become overheated, leading to a self-reinforcing cycle of heat generation and chemical reactions that can end in an explosive failure of the battery.

In a lithium-ion battery, thermal runaway can be triggered by a variety of factors, including:

1. **Overcharging:** When a lithium-ion battery is overcharged, it can generate excess heat and cause the battery cells to break down, which can lead to thermal runaway.
2. **External heat sources:** If a lithium-ion battery is exposed to high temperatures, such as from a fire or other external heat source, it can also trigger thermal runaway.
3. **Internal short circuits:** If the internal components of a lithium-ion battery become damaged or degraded, it can cause short circuits within the battery cells, which can generate excess heat and lead to thermal runaway.

Once thermal runaway is triggered in a lithium-ion battery, the heat generated can cause the battery to rupture or explode, releasing toxic chemicals and potentially causing a fire. This can be dangerous, especially in situations where the battery is located in a confined space or in close proximity to other flammable materials.

To prevent thermal runaway in lithium-ion batteries, it is vital to uphold safe operating temperatures for the battery cells, and to implement safety mechanisms to prevent overcharging or other conditions that can trigger thermal runaway. This can include the use of thermal management systems, such as liquid cooling or passive thermal management, as well as safety features such as battery management systems (BMS) that monitor and control battery performance.

1.7 Problem Definition and aim:

A lot of research has been done for constant discharge process of lithium-ion batteries, but study on thermal behavior of lithium-ion batteries during operation under realistic cycles is scarce. So, the main aim of this study was to better understand the temperature variation of a lithium-ion battery cell when it is charging/discharging.

This study also wants to analyze the thermal behavior of the battery pack during discharge under combined charge and discharge cycles.

1.8 Objectives:

1.8.1 Main Objective:

The main objective of this study is to conduct temperature analysis of electric vehicle lithium-ion cell/ battery during discharging, and combined cycle using ANSYS.

1.8.2 Specific Objectives:

- To find out temperature contour of cell during constant discharge (with or without cooling)
- To evaluate temperature plots during charging/ discharging cycle with or without cooling
- To analyze temperature change in laboratory conditions

1.9 Limitations of the Study:

- The experimental tests were only done for cell at 0.3 C-rate as the maximum current that could be discharged was about 15A.
- The temperature measured by the infrared thermometer could be faulty
- The test was conducted at atmospheric condition without coolants, so effect of coolants on temperature change couldn't be observed
- Simulation was done using NTGK parameters and not the battery parameters of the actual cell which could cause same deviation in the data.

CHAPTER TWO: LITERATURE REVIEW

As mentioned earlier, lithium-ion batteries have some weaknesses that can lead to serious harm to individuals and objects if not used and managed appropriately within safe temperature ranges. (Reis, Strange, Yadav, & Li, 2021) noted in their study that although there is a considerable and expanding collection of lithium-ion battery data available, it is frequently dispersed across various sources and can be challenging to obtain and assess. The paper additionally highlights certain obstacles and constraints associated with utilizing lithium-ion battery data, including the necessity for consistent testing methods and the complexity of generalizing data from laboratory tests on a small scale to commercial batteries on a large scale

(Pesaran A., 2013). discussed that a battery provides optimum performance when it operates between 15 °C and 35 °C and this is recommended. When operated at temperatures outside this range, it can result in significant capacity loss. (Motloch, et al., 2002) found that as the working temperature of a cell increases in the temperature range of 30–40 °C , it decreases the calendar life of the battery immensely. Also, as the temperature exceeds further thermal runaway might occur that lead to a terrible catastrophe (Sun, et al., 2016). In addition, the battery pack works efficiently when the maximum temperature difference among cells and modules in the battery pack is less than 5 °C (Pesaran, 2002). The foremost concern while developing electric vehicles is safety, and it is essential to incorporate an efficient BTMS in Li-ion based EVs, HEVs, and PHEVs to quickly dissipate the heat generated within the battery pack. Diagnostic methods that are effective for Li-ion batteries are crucial to guarantee that they function within the specified voltage and temperature range to prevent untimely deterioration and breakdown (Owen, Robinson, Weaving, & Pham, 2022).

When lithium-ion batteries are charged or discharged, they produce heat which is mainly transferred from the internal part to the surface of the battery and then released into the environment by means of an effective thermal management system such as ambient air or other coolants. The remaining energy is stored within the battery. Therefore, creating

thermal models of batteries involves selecting appropriate equations, such as those for energy balance, heat generation, and boundary conditions (Liua, Weib, He, & Zhao, 2017). In an article by (Yang, Patil, & Fahimi, Jan. 2019), the electrochemistry of batteries is described and the relationship between battery internal parameters, temperature, and current rate is analyzed based on their electrochemical properties. The equivalent circuit model is then used to predict battery behavior under different drive cycles, and the impact of drive cycles on battery performance in electric vehicles is discussed. It is noted that drive cycles with high power requirements generate heat quickly and can lead to potential thermal issues, while milder drive cycles can alleviate thermal stress.

In a paper by (Panchal, Mathew, Fraser, & Fowler, 2018) developed a mathematical model to predict voltage distributions and transient temperature variations in a 18650 cylindrical lithium-ion battery under various discharge rates. In order to furnish quantitative insights into the thermal characteristics of lithium-ion batteries, an air cooling method was employed to conduct laboratory tests on the 18650 cylindrical lithium-ion battery cell. Four thermocouples were affixed to the battery surface to measure constant current discharge rates of 1 C, 2 C, 3 C, and 4 C. Subsequently, a numerical model was formulated using ANSYS, and the outcomes demonstrated that the model's predictions for temperature and voltage aligned well with experimental data. The findings indicated that elevating the C-rates led to a corresponding increase in the battery's temperature.

(Akturk, Yildiz, & Arıcı, October 2021) investigated the thermal efficiency of an electric vehicle (EV) lithium-ion battery module designed for the WLTP Class 2 test procedure. The research commenced by verifying the precision of the model cell and proceeded to construct and simulate a battery module comprising 20 cells arranged in series. The simulation encompassed three distinct cooling rate profiles aligned with driving cycle characteristics, incorporating low, moderate, and high-speed segments. Assessment of the module's thermal performance involved analyzing temperature gradients and reference points along the cell wall positioned in close proximity to the maximum and minimum temperatures.

(Qasmi, Afzal, Nadeem, & Hossain, October 2022) developed a computer model employing ANSYS/Fluent to examine the temperature distribution within a li-ion pouch

cell. The model underwent validation through a 1C discharge cycle, revealing hot spots along the lateral sides of the cell. Internal heat generation increased as temperature decreased and Crates increased. The research emphasized the necessity of a cooling strategy to prevent an undesirable temperature peak exceeding 50°C, especially in scenarios where the cell is exposed to external temperatures exceeding 45°C. These findings underscore the critical role of modeling in tracking temperature distribution and ensuring the safety of batteries, highlighting the importance of Li-ion battery modeling to prevent thermal runaway and ensure overall safety.

(Vikram, Vashisht, & Rakshit, November 2022) examined the thermal dynamics and operational efficacy of a liquid-based thermal management system for a Li-ion battery pack in an electric vehicle across diverse driving cycles and coolant options. Employing numerical simulations on a battery pack consisting of four modules, the results indicated that higher ambient temperatures extended the cooling duration of the thermal management system and escalated cumulative energy consumption. The study further revealed that the optimal performance was observed with a Water-Propylene glycol mixture featuring a 25% concentration of propylene glycol and a Water-Ethylene glycol mixture with a 50% concentration of ethylene glycol.

(Amini, Özelci, & Tanılay Özdemir, June 2020) examined the thermal dynamics of Panasonic NCR18650B cylindrical Li-ion battery cells under the influence of driving cycle loads. The study evaluated how the Li-ion cell responds to the FTP driving cycle at varying operational temperatures. The results underscore the substantial impact of operational temperature on the thermal behavior of Li-ion batteries. Specifically, lower temperatures were observed to induce a noteworthy increase in heat generation and surface temperature, attributed to a rise in internal resistance. Cold ambient conditions were also associated with a significant decrease in the cell's volumetric energy density and capacity, potentially due to reduced ionic conductivity within the cell. This discrepancy between the battery cell surface and ambient temperature becomes more pronounced as the ambient temperature decreases.

In a study by (Vyroubal, Kazda, Maxa, & Vondrák, 2015), the authors investigate the feasibility of using numerical simulation to predict temperature changes during discharge of a li-ion battery. They developed a numerical model using ANSYS Fluent and SolidWorks software and compared the results to real measurements obtained through electrical impedance spectroscopy and thermal imaging. The simulation was conducted in real-time, with a relative error of 1.23%. The authors found that the MSMD numerical model provided relatively high accuracy results with a fast calculation speed of a few minutes. However, the computational mesh quality greatly affected the computational time and accuracy, with finer and higher-quality meshes leading to more accurate results

In another study by (Dhakal, Parameswaran, Muthukumar, & Moussa, 2022), using MATLAB/Simulink, the authors created and simulated a more generic and widely used BTMS system. The battery and BTMS system specifications were chosen based on a case study of popular electric vehicles on the market and previous literature reviewed. The simulation result depicts the fluctuation in energy usage and battery temperature of the cars under various operation situations. The simulation results suggest that BTMS is critical for managing and controlling the thermal behavior of the battery in an electric vehicle.

2.1 EV Challenges and Opportunities in Nepal

The Nepalese government places a greater emphasis on addressing essential needs rather than embracing electric vehicles (EVs). Despite initial enthusiasm and efforts, the anticipated success of EVs has not materialized as planned. The introduction of electric vehicles in Kathmandu commenced with the Trolley bus and SAFA Tempo, but technological, operational, and policy challenges led to the impracticality of SAFA Tempo in the market.

Subsequently, various brands entered the Nepalese market, importing and selling EVs with advanced technology, fostering competition and increasing EV adoption. By 2018, the country had over 41,000 EVs, but sustaining and expanding this growth requires significant efforts to transition the entire nation to a cleaner transportation mode.

Several challenges hinder the widespread adoption of EVs in Nepal. Firstly, the cost of car ownership in Nepal is prohibitively high due to factors like elevated taxes, customs duties, import expenses, maintenance, and fuel costs. The absence of domestic EV producers further complicates matters, making it challenging for middle-class families to afford these vehicles.

Secondly, unclear and ambiguous regulations on the import and operation of electric vehicles in Nepal pose obstacles. While the government has provided certain incentives such as waived road taxes and customs duty discounts, intricate laws and substantial levies categorizing EVs as luxury items impede their market penetration.

Thirdly, power availability is a significant concern, with EV charging stations requiring 6 kW to 22 kW of electrical power. Charging times in Nepal range from 1 to 12 hours, and as the number of EVs increases, there will be a corresponding surge in national energy consumption, creating challenges for the electrical industry. Addressing this issue necessitates the implementation of effective measures and policies by the Nepal Electricity Authority (NEA).

Moreover, the scarcity of charging stations, particularly in rural areas, limits long-distance EV driving. High installation costs result in only a few privately-owned charging stations in large cities. Consequently, vehicle owners often resort to traditional charging methods at home or offices with low ratings, hindering the viability of long-distance EV travel.

Lastly, due to governmental and infrastructural limitations, EVs seem more practical for urban areas than for rural or long-distance journeys. Imported EVs also exhibit limitations, such as conventional designs and subpar torque, rpm, and range specifications, making fossil-fueled vehicles more attractive to buyers.

2.2 Introduction to C-rate

Batteries employed in electric vehicles experience more demanding use compared to those in traditional vehicles. Drivers strive to optimize their usage during road trips and expect rapid charging when the battery is depleted. Nevertheless, frequent and strenuous usage patterns contribute to a gradual reduction in battery capacity over time. While smartphone batteries typically have a lifespan of only a few years, electric vehicle (EV) batteries must endure for a decade or more.

The cycle life of a battery can be compared to the distance it needs to cover—spanning hundreds of thousands of miles over numerous years, serving as a test of its overall endurance. Conversely, its power and charge rate are similar to the speed at which it covers that distance. For electric vehicles to be practical for drivers, their batteries must demonstrate a balanced combination of speed and endurance.

Battery scientists commonly use the term "C/3 cycling," indicating a testing process where the battery is charged in three hours and then discharged at an equivalent rate. This method aims to simulate freeway driving conditions with a moderate recharge rate. However, in real-world situations, drivers seek the ability to cover long distances rapidly, necessitating even quicker recharging times. (Holme, n.d.).

A comprehensive assessment of a battery's performance, encompassing both power and lifespan, is conducted through the 1C test. This test involves charging and discharging the battery within an hour, a pace three times quicker than the C/3 test. In this study, the focus is on evaluating battery temperature during discharge under different rates: 0.3 C-rate, 1C-rate, and 3C-rate (fast charging). The aim is to examine how temperature variations manifest in the cell under these specific charging and discharging conditions.

2.3 Types of Battery Configuration used in Electric Vehicles:

The battery system integrates numerous cells and control electronics into a complete battery that powers the electric vehicle (EV).

Battery Arrangement

In the context of an electric vehicle (EV), battery configuration refers to how individual battery cells are arranged within the battery pack. The selected battery configuration can have an impact on factors such as capacity, voltage, power output, and the overall performance of the vehicle.

The widely used configuration for EV batteries is the series-parallel hybrid configuration. In this arrangement, cells are linked in series to increase the battery pack's voltage, and sets of series-connected cells are then connected in parallel to enhance the overall capacity of the battery pack.

The series connection of cells raises the battery pack's voltage output, which is crucial for generating the necessary power to propel the vehicle. Simultaneously, the parallel connection of groups of cells increases the battery pack's capacity, essential for storing the energy needed to achieve the desired driving range.

Manufacturers typically configure the packs to operate at approximately 400 volts or 800 volts. The specific battery configuration chosen for an EV is influenced by various factors, including the desired range, power output, and the overall weight of the vehicle.

Table 1 Battery configuration information of some Electric Vehicles (400-800 V) (evkx, n.d.)

Model	Gross Capacity	Configuration	Nominal Voltage
Audi Q8 e-tron	116kWh	108s4p	396 Volt
Audi e-tron GT	93.7kWh	198s2p	725 Volt
Kia EV6 GT	77.4	192s2p	697 Volt
<u>Nio 100KWh Battery</u>	100kWh	96s1p	358 Volt
<u>Nio 100KWh Battery</u>	100kWh	96s2p	358 Volt
<u>Mercedes EQE</u>	120kWh	108s4p	328 Volt
<u>Mercedes EQS</u>	120kWh	108s4p	396 Volt

<u>Tesla Model Y Long Range</u>	78.1kWh	96s46p	357 Volt
---------------------------------	---------	--------	----------

2.4 Coolants

To determine which coolant had the optimum cooling performance in BTMS, three types of coolant were examined and evaluated. Along with the water cooling, two conventional coolants—air and 3M Novec 7100—were also simulated. This method has produced a reasonable comparison and made it possible to evaluate the efficiency of the coolants.

Coolant	Air	Water	3M Novec 7100
Density (kg/m ³)	1.225	998.2	1510
Viscosity (kg/m.s)	1.79×10^{-5}	0.001003	6.0×10^{-4}
Thermal Conductivity (W/mK)	0.025	0.6	0.069
Specific Heat (J/kg · K)	1006.43	4182	1183

Cooling lithium-ion batteries (LIB) in a cold ambient environment can be achieved through forced convection using air, wherein the fluid directly contacts the LIB cells. Air cooling is straightforward, cost-effective, and the most convenient for maintenance, as it does not necessitate indirect cooling. Nevertheless, the system's efficiency is compromised due to the relatively low heat capacity of air. (Huber, 2015).

Some studies, such as (Teng, 2012) , have developed methods of increasing efficiency by adding fins or by optimizing the fan speed to ensure maximum cooling is achieved. Therefore, to counter the elevated pressure drop, there is a requirement for increased fan power, an aspect that is suboptimal in a hybrid electric vehicle (HEV). However, it's worth noting that air-cooling may be the less efficient option due to its limited thermodynamic properties, particularly in terms of density, thermal conductivity, and specific heat. (Mansour Al Qubeissi, 2022).

3M Novec serves as a coolant in various electronic applications, including computer processors. In recent times, it has been employed for the direct cooling of Battery Thermal Management Systems (BTMS) owing to its dielectric properties and exceptional fire resistance (Junchao Zhao, 2021). On the other hand, the disadvantage of using 3M Novec in H/EV is its high density.

CHAPTER THREE: RESEARCH METHODOLOGY

Research methodology is a specific technique to identify, select, process and analyze information about the research problem. It illustrates the process and methods applied for the study of the selected topic. It consists of all the sequential steps adopted by the researcher in studying the subject matter.

3.1 Literature Review:

A literature review is a synopsis of the available research for a specific scientific topic. It includes studying and trying to understand all the available text in this topic. Literature reviews summarize existing research to answer a review question, provide the context for new research, or identify important gaps in the existing body of literature. It is the first step in the research methodology. It will be accompanied with the help of different books, reports and research articles.

Literature review is the first and foremost step in the process of understanding the current scenario regarding the electric vehicle batteries and the recent progressions in this field. The main tasks that shall be completed during this phase of work are listed below:

- Literature review from current research articles about EV batteries, battery thermal management system(bms), drive cycles
- Literature review about why electric vehicles is replacing diesel, petrol engine vehicles
- Literature review about the different btms practices prevalent across the world
- Literature review about the effect of various coolants in cooling the batteries

3.2 Conceptual Framework:

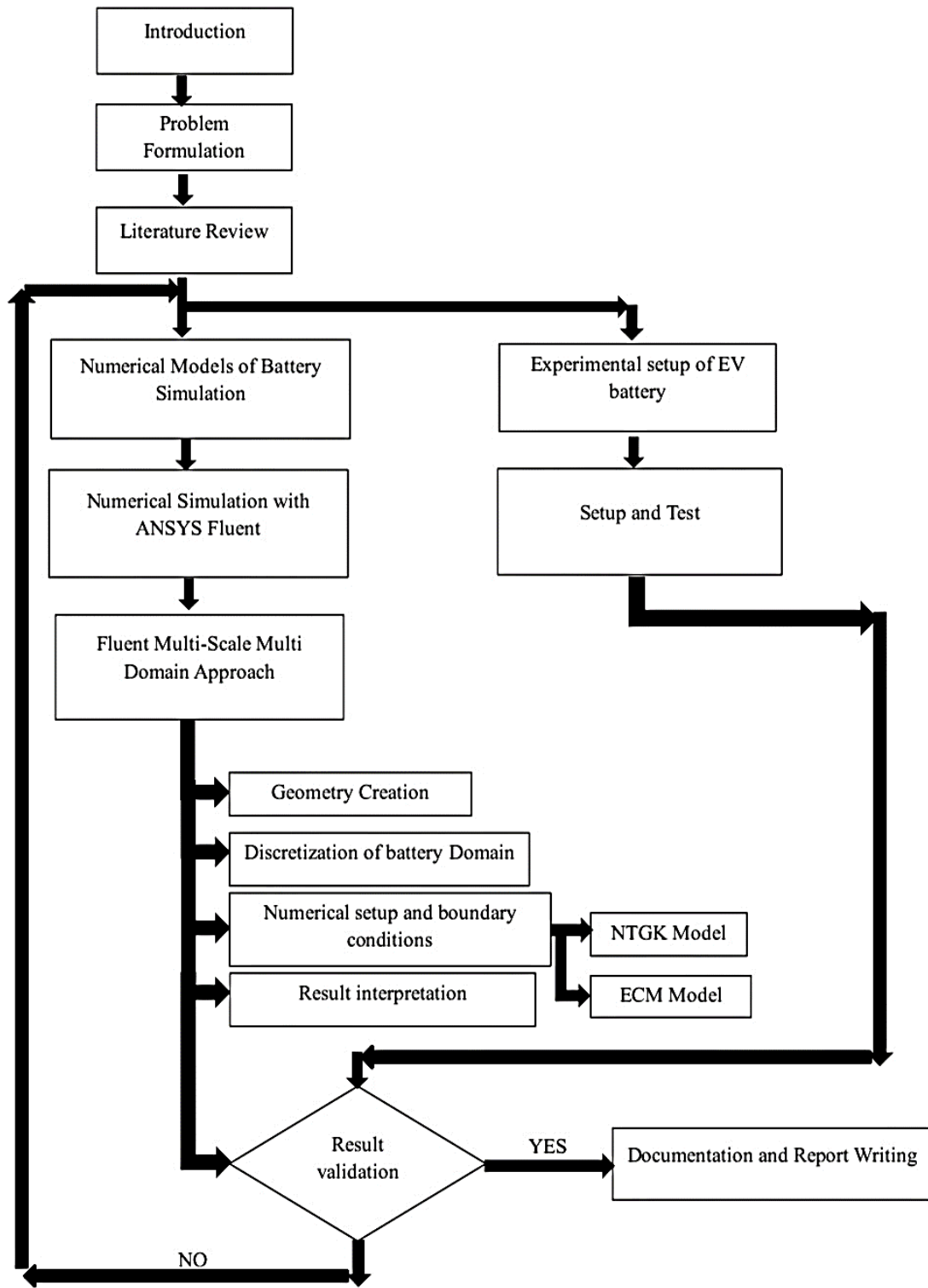


Figure 3 Conceptual Framework

3.3 Experimental Setup

After the preparation of conceptual framework, the considerations for the experimental setup are designed. After selecting the appropriate battery, the equipment required for carrying out the experiment are finalized. The operating conditions were analyzed to determine the experimental conditions. Along with temperature measurement of the battery when discharging, the voltage and current behaviour were also observed.

3.4 Analytical Design of the cell

The first step includes designing the geometry of the cell. Two different cells will be designed in ANSYS. The first is LG Chem cell which is widely simulated in various literatures, and another cell is Highstar cell which was used for test. Making use of the dimensions of the LG Chem cell that is available, a single cell model is created and an appropriate series parallel combination of cell is generated. A pack containing three cells with three series connections and one parallel is designed. We will build a module containing three battery cells linked by busbars.

3.4.1 For LG Chem cell:

A 14.6 Ah LIB comprising a LiMn_2O_4 cathode, a graphite anode, and a plasticized electrolyte from LG Chem. was demonstrated in this work (Ui Seong Kim, 2011).

The subject of our study is the geometric configuration depicted in Figure 4, which comprises a module composed of three battery cells. These cells are positioned with a separation of 3 mm between each other and are interlinked by a busbar measuring 2 mm in thickness. The construction of this configuration will be carried out using the ANSYS DesignModeler tool.

For simplification, the geometry of the single cell is first modeled and simulated.

The dimensions of the cell are:

For active zone: 145mm×192mm×2mm

For tab zones: 45mm×45mm×2mm

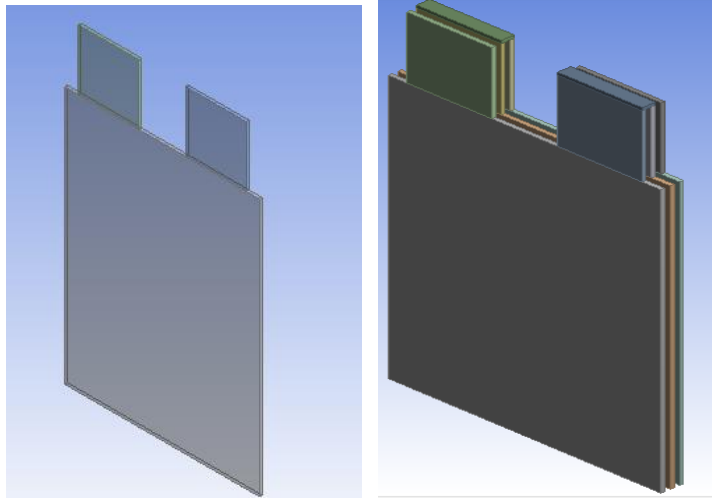


Figure 4 Geometry of single cell and 3s1p battery pack

3.4.2 For Highstar cell:

A 50 Ah LIB comprising of LiFePO_4 cathode was modeled for this work.

The dimensions of the cell are:

For active zone: 185mm×160 mm×36mm

For tab zones: 35mm×28mm×7mm

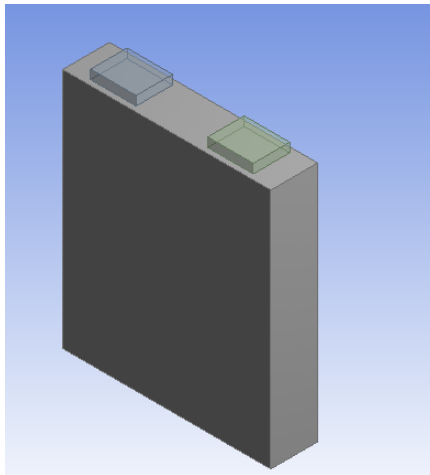


Figure 5 Highstar cell

3.5 Mesh

The Meshing of the domain is done by using the Meshing tool of ANSYS. For simplification, meshing with linear element with size of 0.001m is done. The total number of elements for the single cell is 63780, for battery pack it is 192600, and a representation

of the mesh can be seen in Figure 7. The mesh size for highstar cell was 0.002m and the total number of elements for the single cell of highstar is 135936.

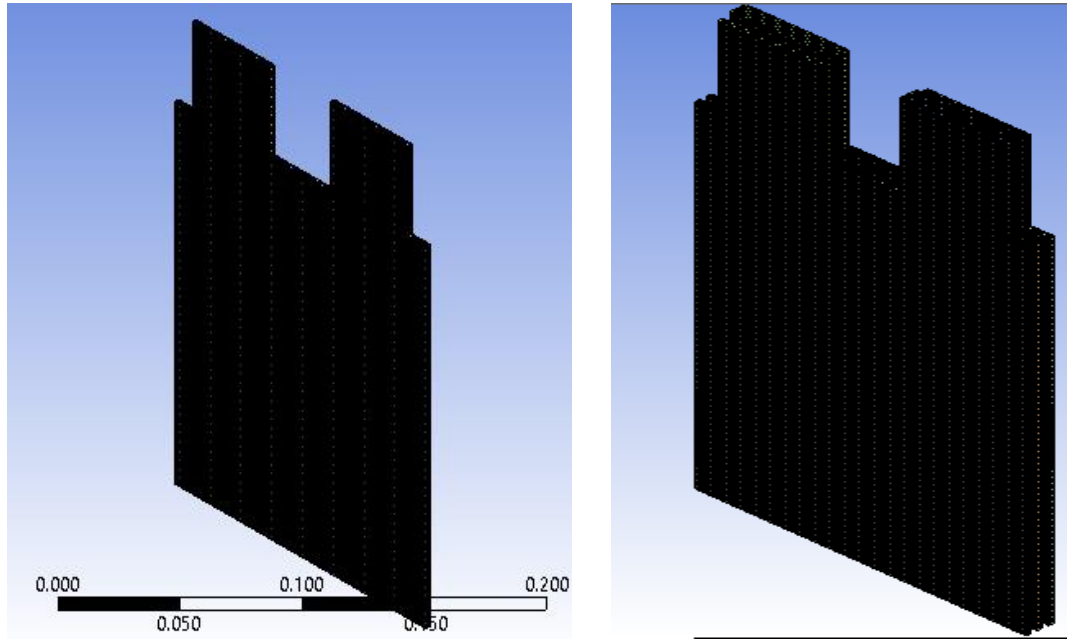


Figure 6 Meshed structures

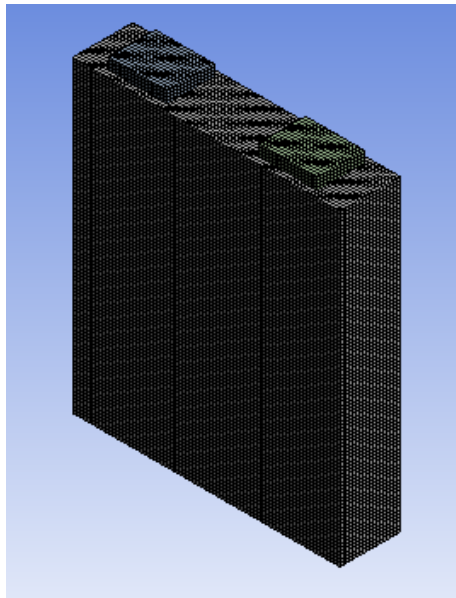


Figure 7 Meshed structure of highstar cell

3.6 Numerical Simulation

After the geometry of the model has been prepared. The next step will be to perform simulation of the battery in Setup of ANSYS fluent. To perform the battery simulation, we use MSMD battery module.

3.6.1 Models of Battery Simulation in ANSYS

The simulation of the electro-thermal cell will be conducted using the Ansys/Fluent platform. To accomplish this, the widely recognized Fluent Multi-Scale Multi-Domain (MSMD) technique will be employed to manage diverse physics within solution domains, specifically the layers of the anode, separator, and cathode. When employing this modeling approach, the electrical and thermal fields of the battery are resolved in the Computational Fluid Dynamics (CFD) domain at the scale of the battery cell through the solution of the following differential equations:

$$\frac{\delta\rho C_p T}{\delta T} - \nabla \cdot (k\nabla T) = \sigma_+ * |\nabla\varphi_+|^2 + \sigma_- * |\nabla\varphi_-|^2 + \dot{q}_{ECh} + \dot{q}_{short}$$

$$\nabla \cdot (\sigma_+ \nabla\varphi_+) = - (j_{ECh} - j_{short})$$

$$\nabla \cdot (\sigma_- \nabla\varphi_-) = j_{ECh} - j_{short}$$

Where σ_- and σ_+ are the effective electric conductivities for the negative and positive electrodes,; j_{ECh} and \dot{q}_{ECh} are the volumetric current transfer rate and the electrochemical reaction heat due to electrochemical reactions, respectively; φ_- and φ_+ are phase potentials for the negative and positive electrodes; j_{short} and q_{short} are the current transfer rate and heat generation rate due to battery internal short-circuit, respectively; in this case not needed (ANSYS, 2015).

The equations to calculate the source terms, $jECh$ and $qECh$, depend on the adopted sub model which can be:

1) NTGK model

This thermal and electrochemical model of the battery module was created with the Newman, Tiedemann, Gu and Kim (NTGK) model (ANSYS, 2015) proposed by Kwon et al. (Kwon, Shin, Kang, & Kim, 2006) and validated by others. Volumetric current transfer rate J (A/m³), which are important parameter used in this model, is calculated by the algebraic equation as given below.

$$J_{\text{Ech}} = a * [U - (\varphi_+ - \varphi_-)]$$

where a is the specific area of the electrode sheet, U and Y are functions of depth of discharge (DOD) and obtained by fitting voltage-current response curves from experiments or provided by the manufacturer.

φ_+ and φ_- denote phase potentials (V) for the positive and negative electrodes. The electrochemical reaction heat, which is an important parameter in our study and affects the temperature increase of the battery module, is calculated as follows:

$$\dot{q}_{\text{Ech}} = J_{\text{Ech}} * (V_{\text{oc}} - V) - J_{\text{Ech}} T * \frac{dV}{dT}$$

where, q_{Ech} is the electrochemical reaction heat (W/m³), J_{Ech} is the volumetric charge or discharge current transfer rate (A/m³), V and V_{oc} represent cell voltage and open circuit voltage (V) respectively, T is also the temperature in K.

3.6.2 Approaches of Simulation:

A series of simulations utilizing the NTGK model with varying configurations were conducted to assess the behavior of each of the examined models.

Subsequent to these simulations, two sets of necessary tests will be executed: firstly, a round of straightforward discharge operations at different C-rates, and secondly, a compound charge/discharge cycle. Each of these approaches will be elaborated upon below.

1. Simple discharge response:

In this stage, a sequence of fundamental discharge processes will be performed. Three discharges with varied C-rates will be simulated for each model: one at 0.3 C, another at 1 C, and a final one at 3 C.

The C-rate, representing how rapidly a battery charges or discharges, is defined as the ratio of the current passing through the battery to the theoretical current at which the battery would provide its nominal capacity in one hour. The chosen battery's nominal capacity is 14.6 Ah, signifying that a current of 14.6 A equates to a C-rate of 1 C and would deplete the battery in 1 hour.

The following variables will be closely monitored:

- **Temperature:** A critical factor in electric batteries, particularly in Li-ion batteries, as a decrease in temperature leads to a decline in the battery's discharge capacity, while a rapid increase may trigger thermal runaway, resulting in catastrophic breakdown.
- **Passive zone potential:** The difference in potential between the battery's positive and negative terminals, which typically decreases with increasing State of Charge (SOC) and rises with elevated temperature.
- **Total heat generation:** The overall amount of heat produced by the battery. This includes Joule heat (generated by the flow of electrons through the battery, also known as irreversible heat), Electrochemical heat (reversible heat), and short-circuit heat.

2. Compound cycle response

The behavior of each cell/module in the presence of rapid changes in electrical load will be studied as the second phase of the study. To do this, a compound cycle comprised of numerous alternating charge and discharge cycles will be prepared, with the goal of substantially simulating the behavior of a battery in an electric or hybrid car, followed by a stable charging process.

The cycle, which is designed as a function of flow time, uses current intensities, C-rates, and powers to calculate charge and discharge rates. It is broken into 9 segments and has a total simulation time of 900 seconds. The cycle has the following elements:

1. Discharged at 200 W for 150 s
2. Charged at 1 C for 40 s
3. Discharged at 1 C for 60 s
4. Charged at 5 A for 60 s
5. Discharged at 5 C for 20 s
6. Discharged at 0.5 C for 100 s
7. Discharged at 100 W for 30 s

8. Discharged at 400 W for 40 s

9. Charged at 1 C for 400 s

To analyze the results, they will be depicted in graphs, with each variable (temperature, voltage, and heat) presented in a separate graph showcasing its relationship with flow time.

3.6.3 Setup

Now that the mesh has been completed and imported into FLUENT, the required conditions are applied to the model. This will be done in accordance with the ANSYS Fluent Tutorial Guide's guidelines. The next step is to add-on the Dual-Potential MSMD battery model to ANSYS Fluent, and enable the energy equation and transient state. After this, the battery model options are defined. Then NTGK parameters are selected for simulation (which is provided default by ANSYS as seen in figure 8. The simulation is done using two different approaches, first is discharge at constant C-rates, and another is charge and discharge using a combined cycle.

1. For Simple discharge

Regardless of the approach that is being used in the simulation, some aspects of the battery model have to be defined.

The nominal cell capacity for LG Chem cells will be set at 14.6 Ah and 50Ah for Highstar cells, and the C-rate will be set. For simple discharge process, this C-rate will remain constant during the simulation. In the conductive zone window, the cell zone is selected at the active component, while the remaining zones: busbar, tabs zones are selected as passive zone. Finally in the electric contact window, the two tabs are specified where ptab represents the positive tab of the cell and ntab represents the negative tab.

NTGK Model Polarization Parameters

Initial DoD	Reference Capacity (ah)		
0.5	10.51		
Data Types			
<input checked="" type="radio"/> Polynomial <input type="radio"/> Table			
U Coefficients			
a0 4.12	a1 -0.804	a2 1.075	a3 -1.177
a4 0	a5 0		
Y Coefficients			
b0 1168.59	b1 -8928	b2 52504.6	b3 -136231
b4 158531.7	b5 -67578.5		
Temperature Corrections			
C1 1800	C2 -0.00095		

Figure 8 default parameter for NTGK

After this, the battery configuration is checked in this MSMD add-on. After it prints the battery configuration as ok, the battery model is fully defined and now the materials will be covered. For the simulation, the three different materials as specified in ANSYS tutorial is used to define the geometry:

1. e-material: This is the solid that defines the property of the active zones (the cells). Here are its properties:

- Specific heat (Cp): 871 J/kg·K
- Density: 2092 kg/m³
- Electrical conductivity: 3.541 e6 siemens/m
- Thermal conductivity: 20 W/m·K

2. t_material: This material is used to define the tab zones(positive tab and negative tab). Most of its properties are same to that of the e_material, except the electrical conductivity which is 1 e7 siemens/m.

3. Aluminium- For the bus bars

Once the materials are defined in the materials tab, the next step involves setting up the boundary conditions. Thermal convection conditions will be imposed on all walls, excluding the tabs (tab n and tab p, which do not undergo heat exchange), with a heat transfer coefficient set at 5 W/m²K and a free stream temperature maintained at 300 K.

The following reports were defined to extract the relevant data for this study. The data obtained from these were displayed as plots and contours.

- Temperature: volume report of Maximum Static Temperature for the cell and tabs.
- Total heat: volume report of Volume Integral of Total Heat Source for whole domain.
- Voltage: surface report of Area-Weighted Average of Potential for the cell zone and the positive tab.

2. For Compound cycle

The proper way to input the combination/ compound cycle to ANSYS is by describing its various components into a txt file. Fluent supports two different types of profile for these kind of simulations. The first is a timed scheduled profile where with flow time the value of the electric load changes. The next profile is an event-scheduled profile where there is a forwarding condition to change from one load to the next.

The way these profiles are presented is also different on the basis of no. of columns. The time scheduled profile has 3 columns in its .txt file while the event scheduled profile has 4 columns (ANSYS, 2015).

The time based profile is used for this simulation and its various columns include:

1. Time
2. Electric load value
3. Type of Electric load type (represented by an integer number)
 - 0: C-rate
 - 1: Current

2: Voltage

3: Power

4: External electric resistance

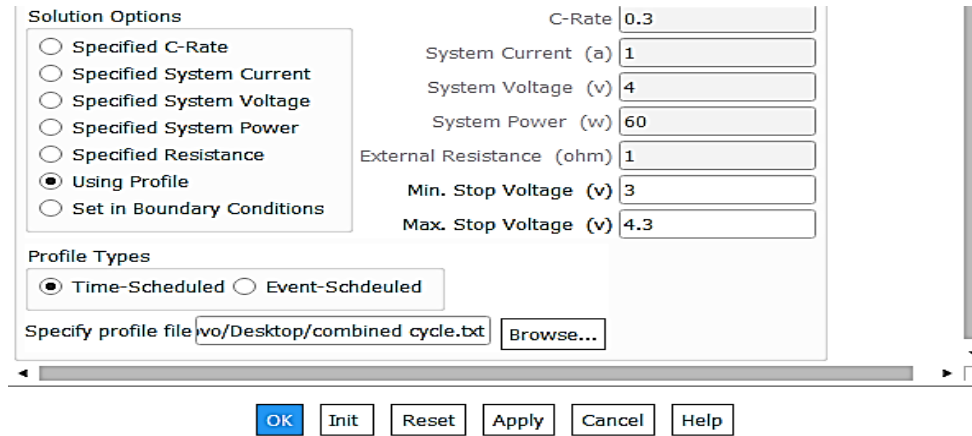


Figure 9 setting for different solution options

Therefore, to translate the time profile described earlier, the .txt file that has to be built as shown in figure below:

p	200	3
150	200	3
150.1	-1	0
190	-1	0
190.1	1	0
250	1	0
250.1	-5	1
310	-5	1
310.1	5	0
330	5	0
330.1	0.5	0
430	0.5	0
430.1	100	3
460	100	3
460.1	400	3
500	400	3
500.1	-1	0
900	-1	0

Figure 10 Charge/ discharge combination file in .txt

This charge discharge profile can be loaded to fluent by changing the solution option to Using profile from the specified C-rate option. After this we simply load this profile in txt form to ANSYS and the simulation is performed.

Boundary Conditions:

For simple discharge/ compound cycle simulations, thermal conditions for wall were set with convection coefficient as 5W/m2-k and 300K wall temperature.

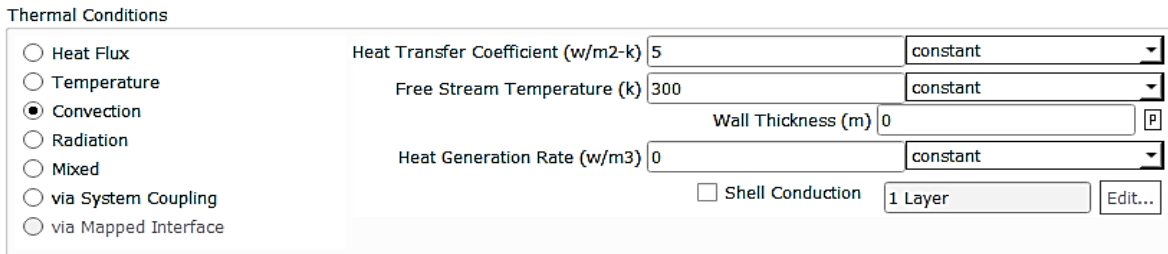


Figure 11 thermal conditions

For simulations with cooling fluid (namely-air, water, 3M Novec 7000), the velocity was specified for the inlet and pressure for the outlet.

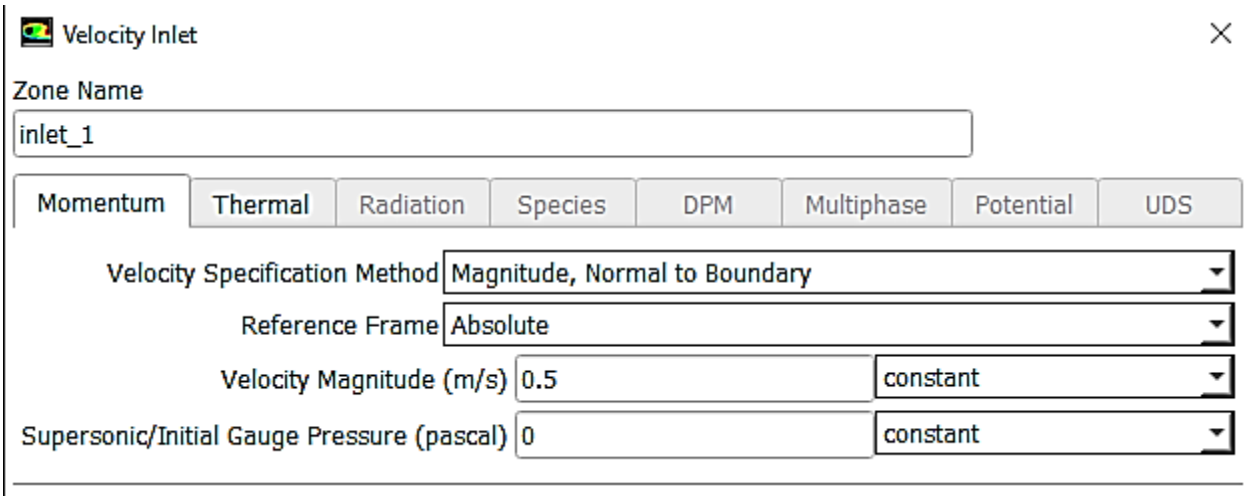


Figure 12 Boundary condition at inlet

Pressure Outlet ×

Zone Name

Momentum
 Thermal
 Radiation
 Species
 DPM
 Multiphase
 Potential
 UDS

Backflow Reference Frame

Gauge Pressure (pascal)

Pressure Profile Multiplier

Figure 13 Pressure specification at outlet

3.7 Result interpretation, conclusion and documentation

This section covers the simulation and experimental work's results and outcomes. Correlating the results with analytical solutions confirms their reliability and validity. A detailed interpretation of the results and data to grasp the physical phenomena by determining the links between the factors involved. The variations and their ramifications are studied, and the conclusion addresses the study questions and makes additional recommendations. The work is recorded from the start of the project to the end of the project after simulation and experimentation. The documentation process, on the other hand, extends beyond the ultimate result and is an ongoing process that is always being improved.

CHAPTER FOUR: RESULTS AND DISCUSSION

4.1 For Single Cell (LG Chem):

4.1.1 For single cell under different discharge rates:

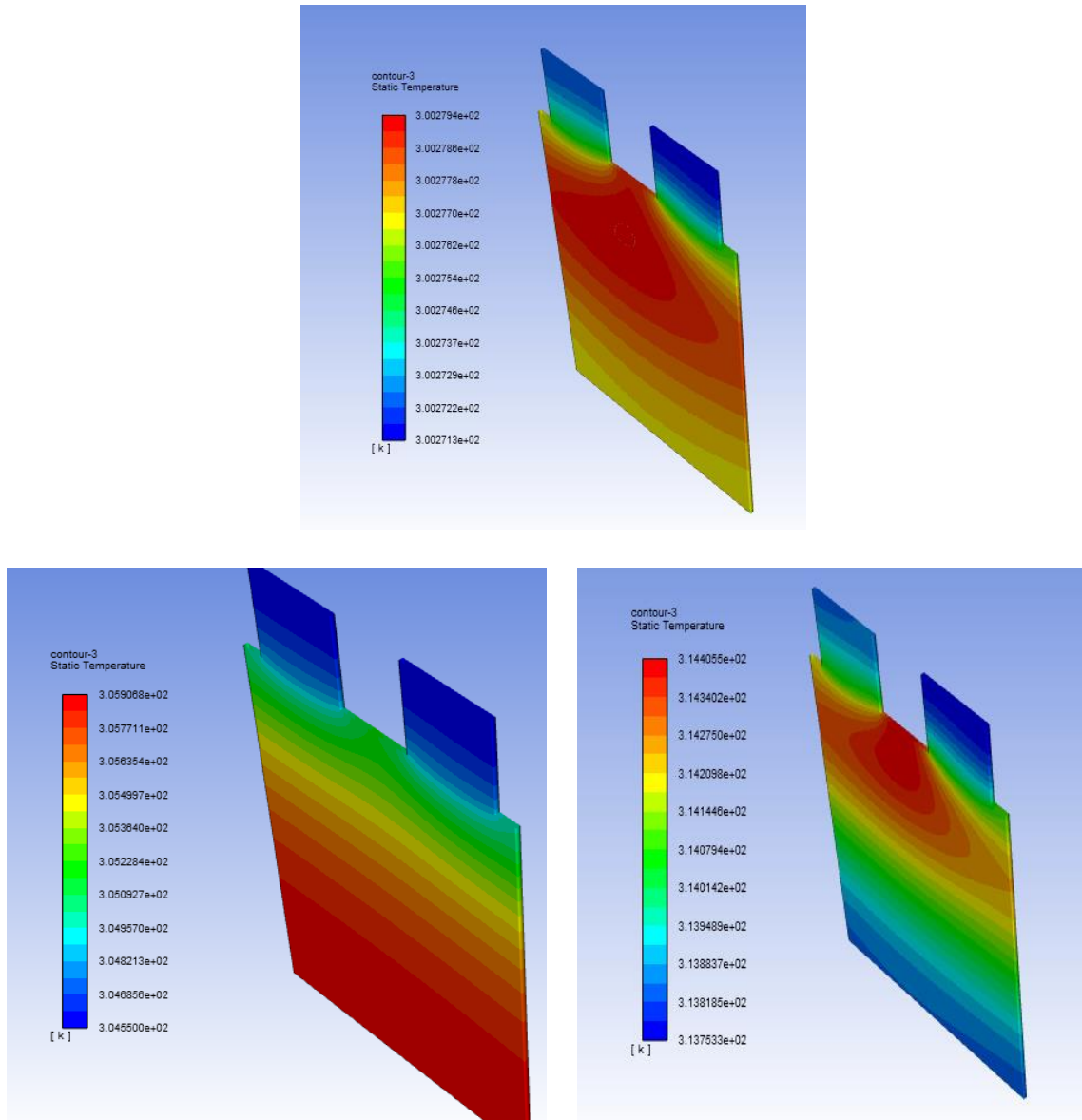


Figure 14 Contours of temperature at 0.3C, 1C and 3C respectively

It was seen that with increase in C rate the temperature of the cell increased drastically. The maximum temperature of 300.2794 K, 305.9 K, 313 K was seen for cells when

simulated with 0.3C, 1C and 3C rate respectively. Whereas for 3C, temperature reached maximum pretty soon. It can be seen that temperature homogeneity across the cell was affected by increasing the discharge rate.

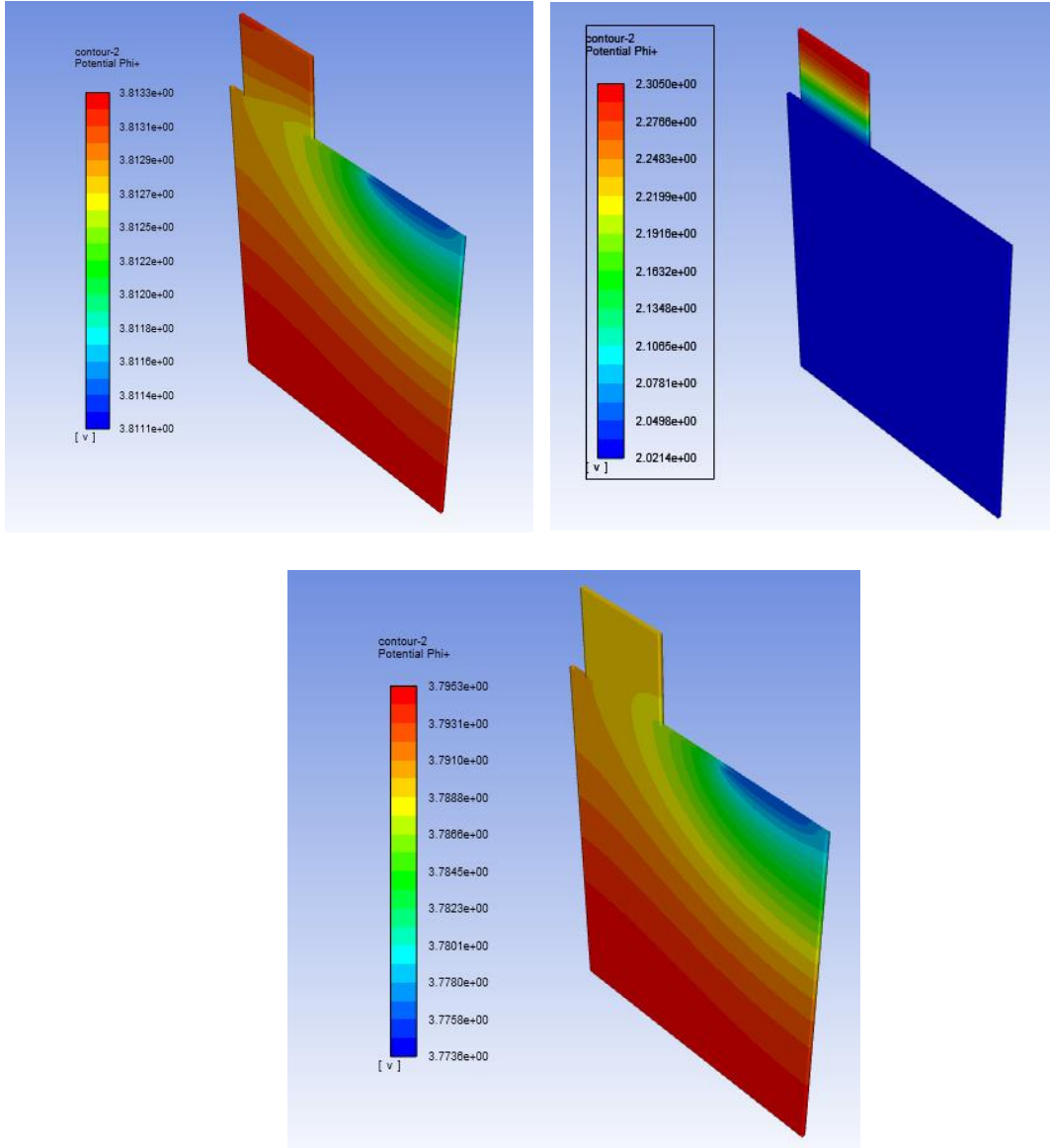


Figure 15 Potential contours at 0.3 C, 1C and 3C

Figure 15 shows us the contours of positive potential at the three different C-rates. It is observed that the value of positive potential is higher at higher C-rates. The values of the positive potential and temperature of the cell from the simulation is derived and it was presented in form of MATLAB plots.

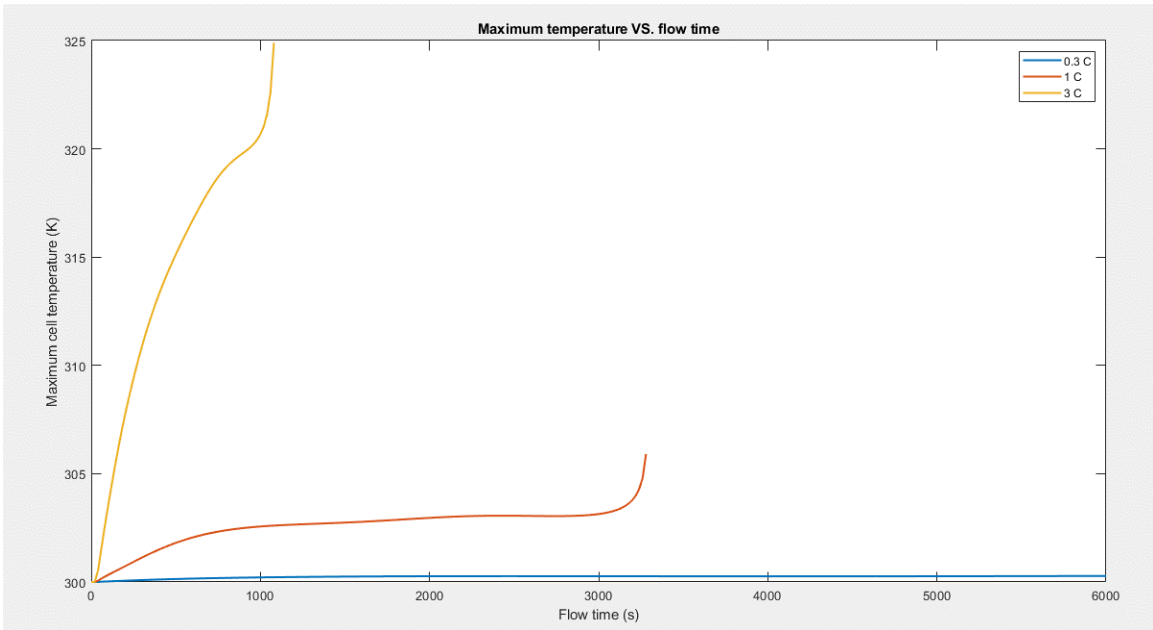


Figure 16 Maximum cell temperature variation for 0.3C, 1 C and 3C

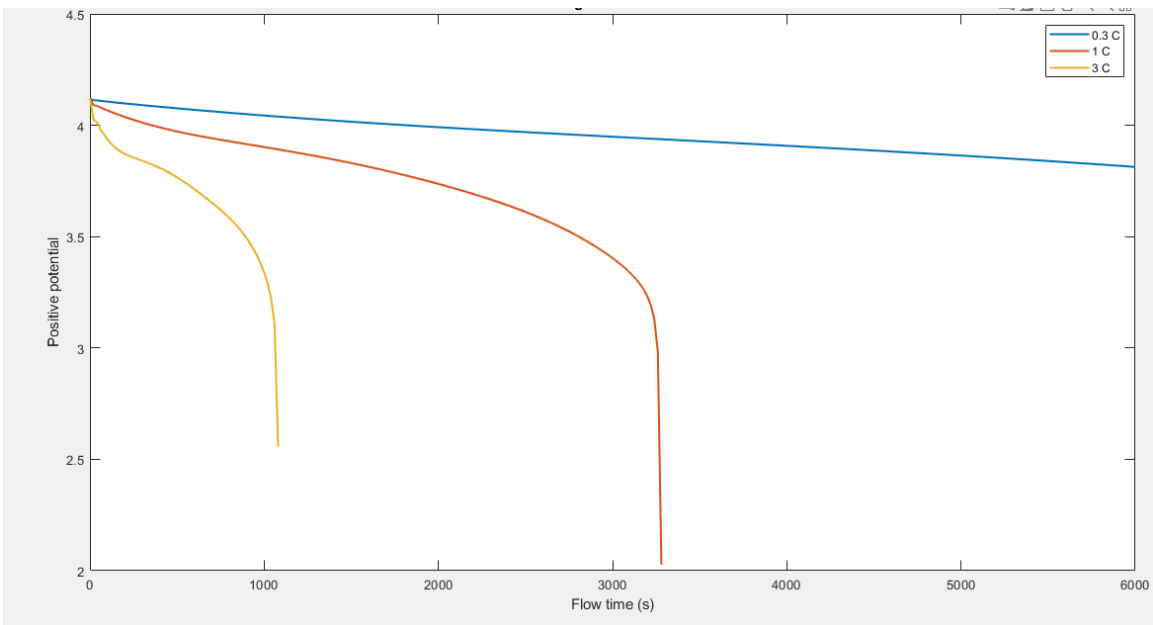


Figure 17 Phi+ plots across the different C-rates

Figure 16 shows how the maximum temperature of a cell increases with increase in C-rates. So, it can be observed that at higher C-rates the maximum cell temperature increases

drastically. Figure 17 helps us understand the fall in positive potential of a cell as the cell undergoes discharge. This plot shows that the potential dips faster at higher C-rates.

4.1.2 For single cell (air cooled) under different discharge rates:

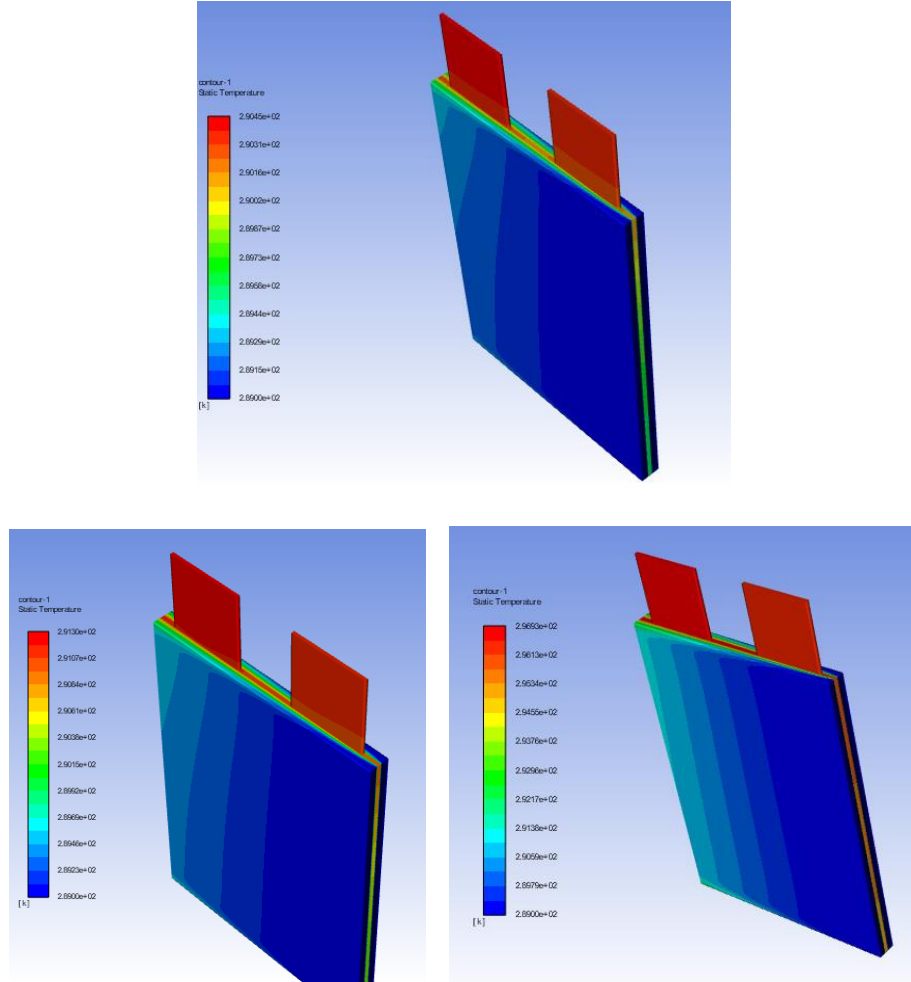


Figure 18 Contours of Temperature at 0.3 C, 1C and 3C respectively

It was observed that the effect of increasing C rate on the cell increased the temperature. The maximum temperature of 290.45 K, 291.30K, 296.9277 K was seen for cells when simulated with 0.3C ,1C and 3 C rate respectively.

4.1.3 for single cell (water cooled) under different discharge rates:

At c rate of 0.3:

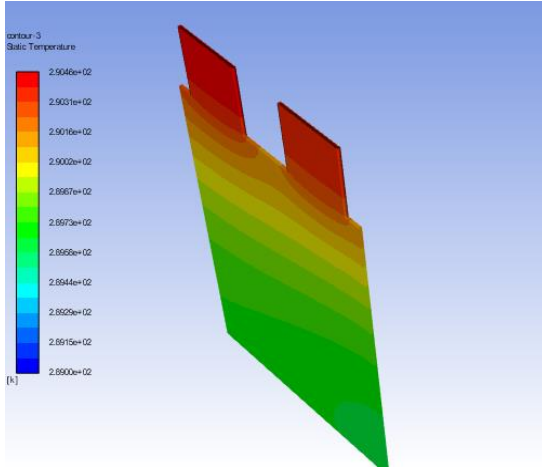


Figure 19 Contours for temperature for c-rate 0.3

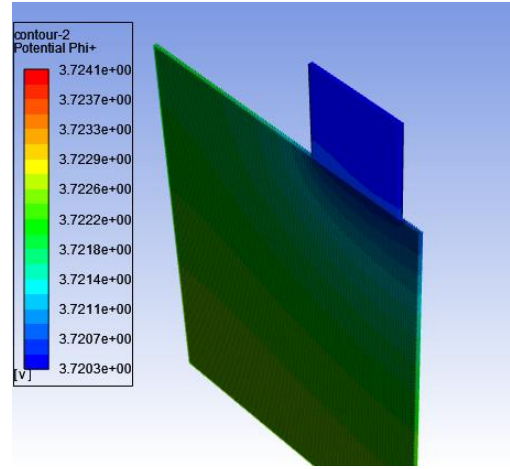


Figure 20 Contour for potential

When the cell is simulated at a c-rate of 0.3, we can see that the heat generated on the cell when it is cooled by a stream of water at 0.5m/s, 289K causes the temperature to rise to about 290.46 K. The maximum temperature occurs at the tab, because the cell zone is cooled by the cooling channel. The minimum temperature that occurs across the surface is 289K. The area weighted average of potential ($\phi+$) was found to be 3.7221812 V.

At 1C:

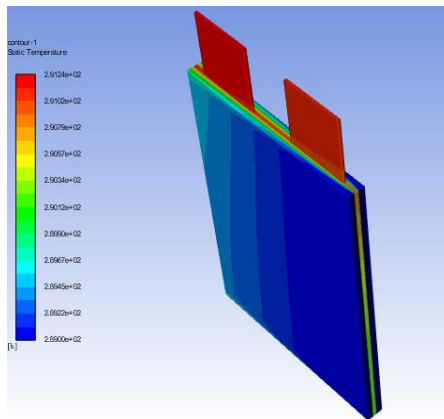


Figure 21 Temperature contour of cell at 1 C

It was observed that the maximum temperature of the cell increased gradually from 289K and was constant at 291.048 K with the minimum remaining constant at 289 K. The temperature of the cell increased due the heat generation in the cell.

At 3C:

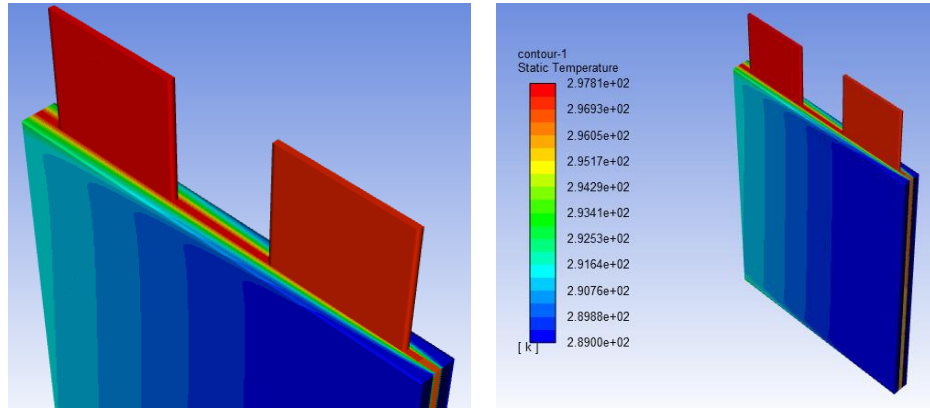


Figure 22 Plots for temperature and temperature contour of water-cooled cell at 3C

From figure 24, we can see that a water cooled cell when discharged at a c rate of 3 with water flowing at 0.5 m/s sets the minimum temperature at 289 K and the maximum temperature that the cell can reach during the cycle is 297.81 K.

4.1.4 For single cell (cooled with 3M Novec 7100) under different discharge rates:

At 0.3C:

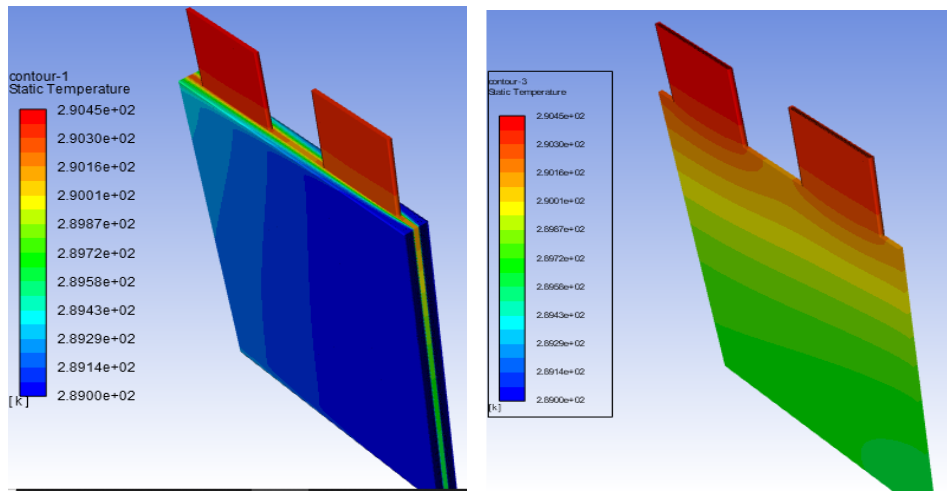


Figure 23 Temperature contour and maximum temperature plots of 3M Novec cooled cell at 0.3 C

The maximum temperature was found to be 290.45 K at the tabs of the cell and the minimum temperature was 289K.

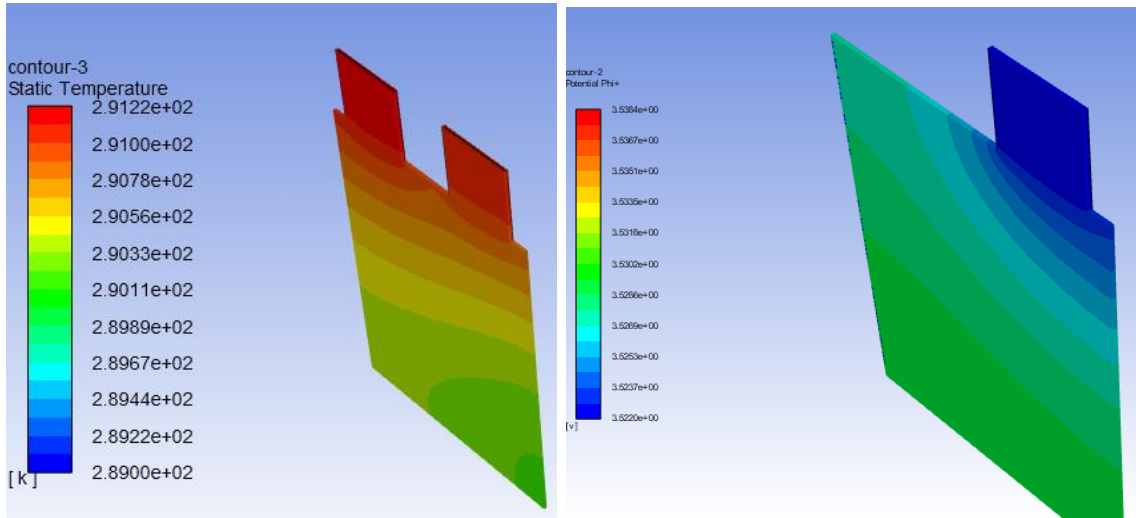


Figure 24 Temperature contour and potential contours of water cooled cell at 1 C

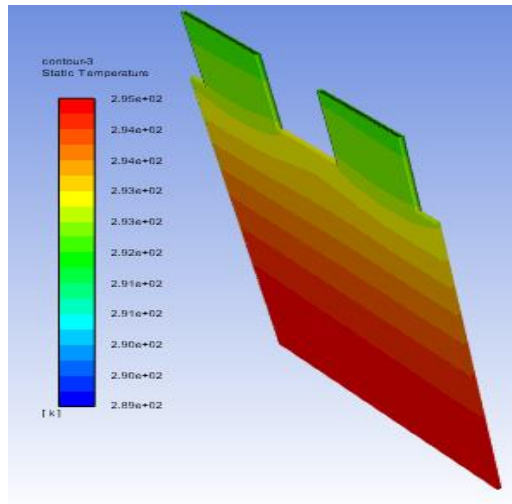


Figure 25 Temperature contour of temperature at 3C for water cooled cell

At 0.3 C, the maximum temperature was found to be 290.45 K at the tabs of the cell and the minimum temperature was 289K. At 1C discharge, the maximum temperature was found to increase to 291.45 K at the tabs of the cell and the minimum temperature was 289K. Similarly, when discharge was 3C, the maximum Temperature reached 295.032 K.

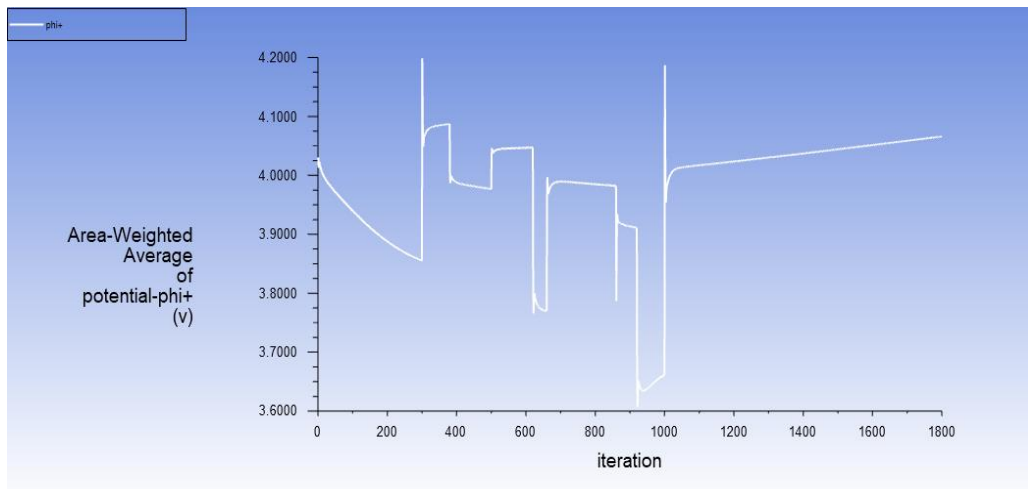
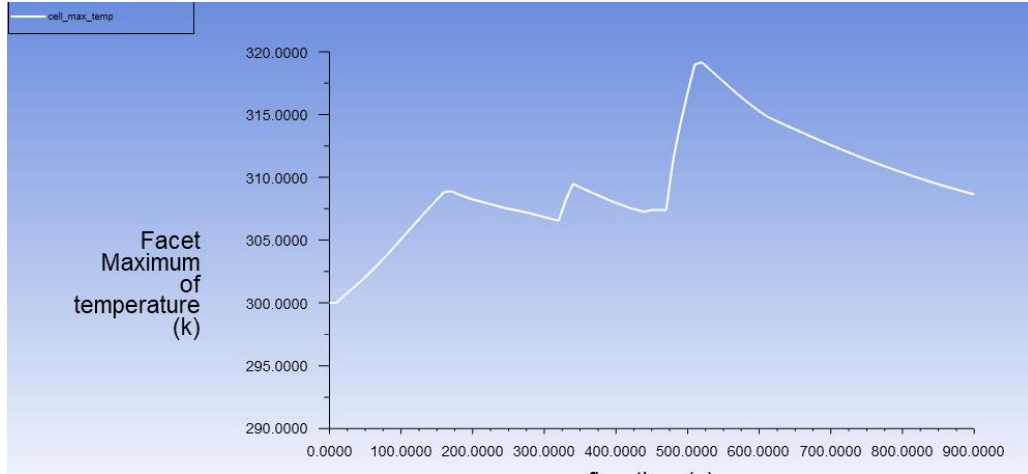
The variation in maximum and minimum temperature of the cell is tabulated below:

Table 2 The temperature variation for single cell with different coolants and discharge rates

SN	Coolant	Discharge rate	Max. Temperature	Min. Temperature
1	-	0.3	300K	300K
	-	1	305.9 K	300K
	-	3	313.29099 K	300K
2	Air	0.3	290.45 K	289K
	Air	1	291.30 K	289K
	Air	3	296 K	289K
3	Water	0.3	290.46 K	289K
	Water	1	291.24K	289K
	Water	3	297.81K	289K
4	3M Novec 7100	0.3	290.45 K	289K
	3M Novec 7100	1	291.22 K	289K
	3M Novec 7100	3	295.032 K	289K

From table 2 and the respective temperature contours for all the cases tabulated above, we can observe that the maximum temperature of the cell when discharged is less for case4, so we can say that the cooling effect produced by 3M Novec 7100 is the best.

4.1.5 for single cell under charge/discharge cycle:



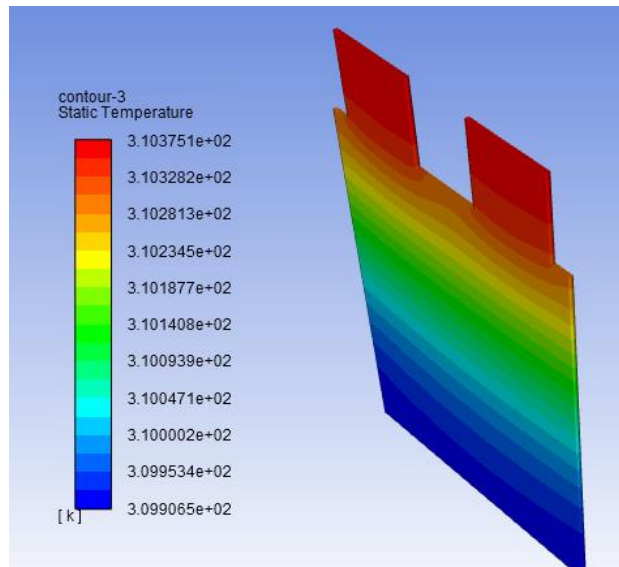
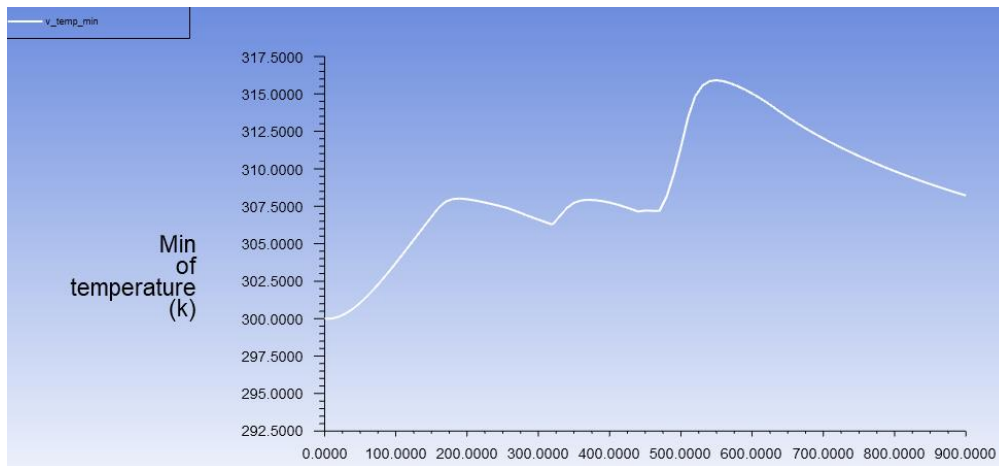
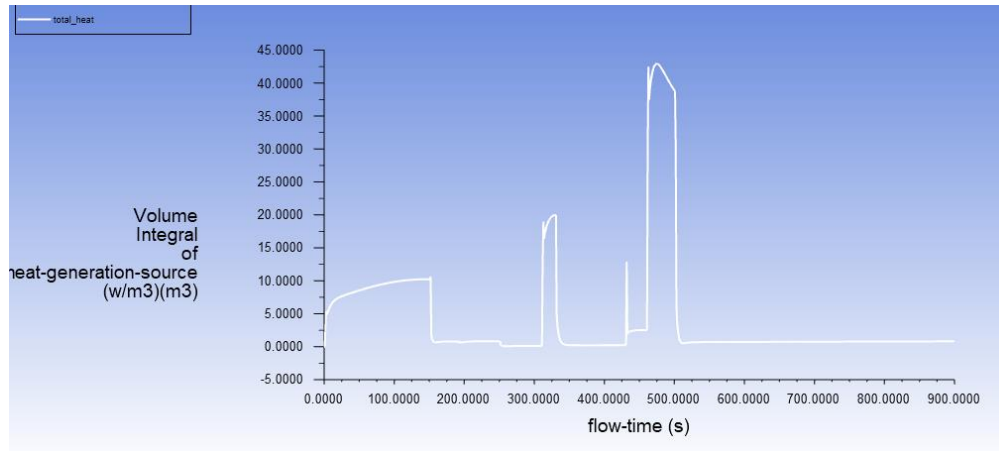
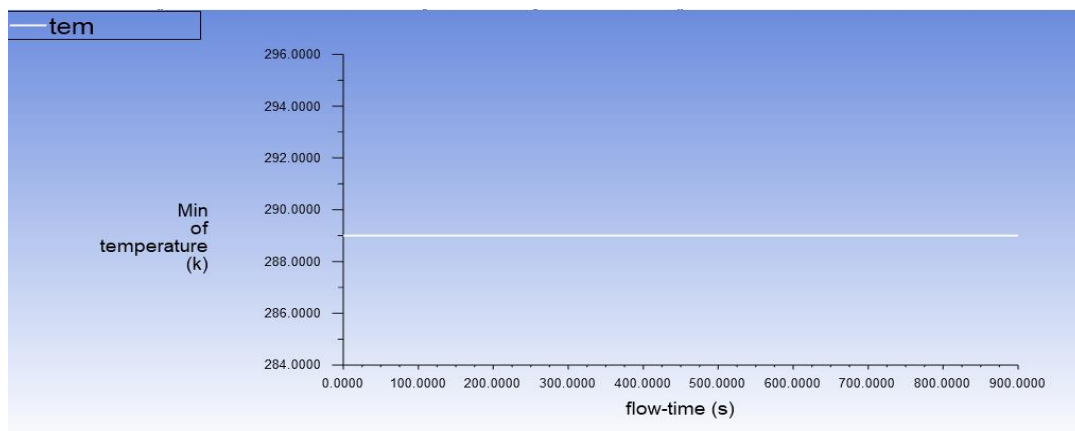
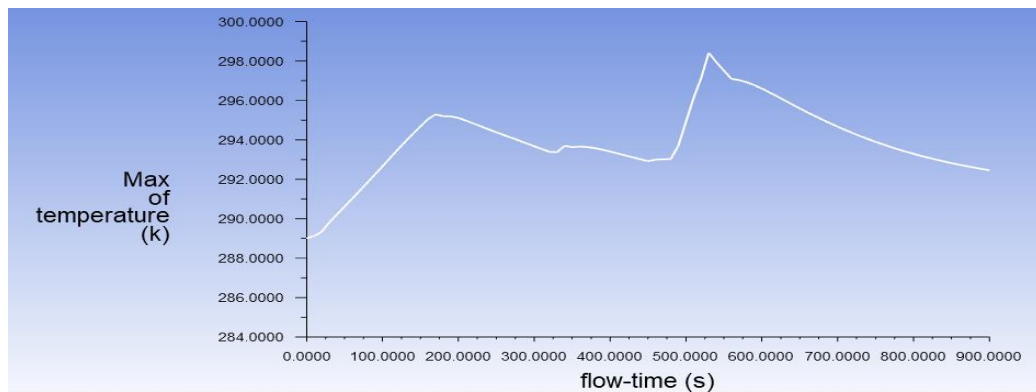


Figure 26 Plots of Maximum temperature, Minimum temperature, and potential for single cell- under charge/discharge cycle

By reviewing the plots in figure 26, it can be found that the maximum temperature increase occurred during the charging of cell at 1 C for 400s, i.e., the 9th component of our cycle. The maximum temperature is found to be 319.5 K. The maximum temperature was observed at the tabs.

Also we can see that the increase in maximum temperature was due to the excess heat generation during the charging of cell in the 9th component of the cycle. It can also be seen that the potential of the battery decreases during the discharge processes and increases during the charging processes. But the volume of heat generation across the cell increases during discharge and decreases during charging processes.

4.1.6 for single cell (air cooled) under charge/discharge cycle:



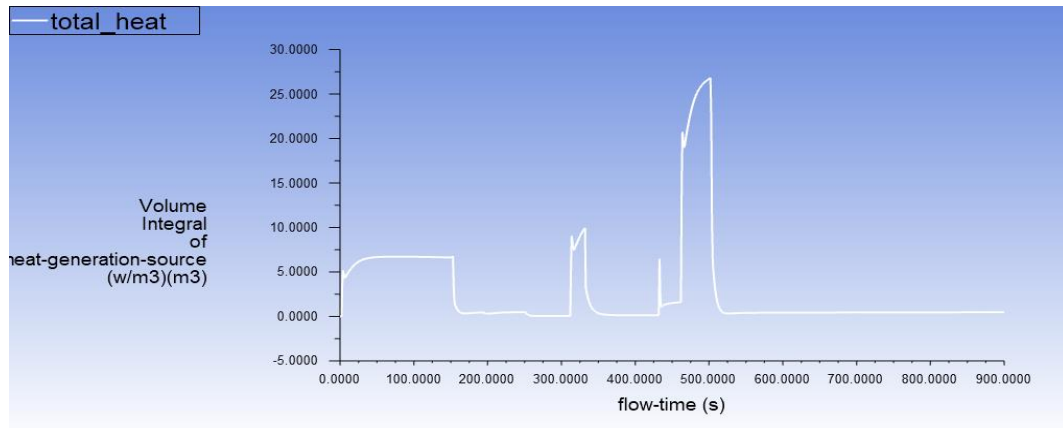


Figure 27 Plots of Maximum temperature, Minimum temperature, and potential for single cell- under c/d cycle (air cooled)

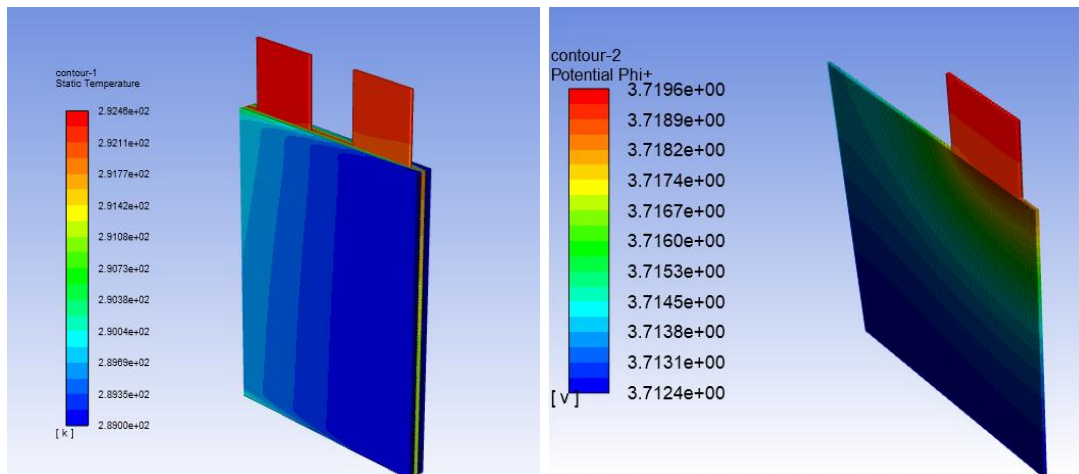


Figure 28 Contours for temperature and potential across the cell

From the figures 27 and 28, we can see that an air-cooled cell with air flowing at 0.5 m/s sets the minimum temperature at 289K and the maximum temperature that the cell can reach during the cycle is 298.41 K.

4.1.7 for single cell (water cooled) under charge/discharge cycle:

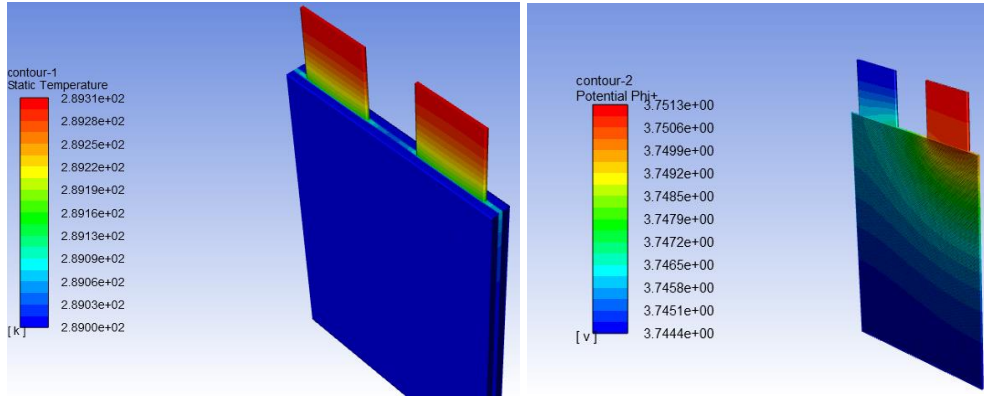


Figure 29 contours for potential and static temperature of water cooled cell

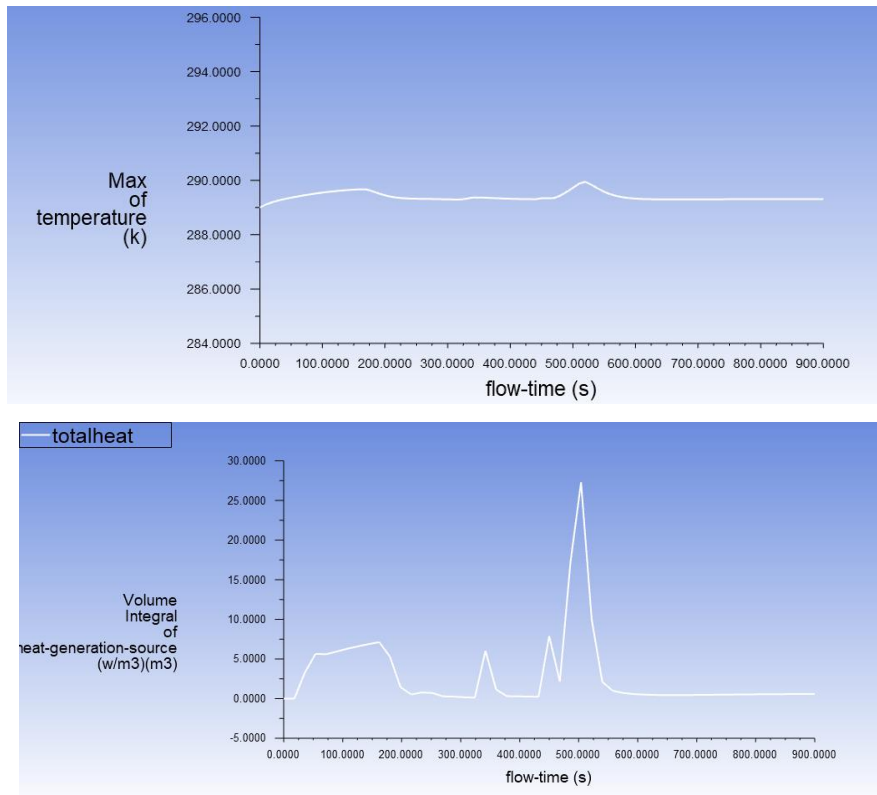


Figure 30 Plots for maximum temperature and total heat generation

From the temperature contour in figure 30, we can see that a water-cooled cell with water flowing at 0.5 m/s sets the minimum temperature at 289 K and the maximum temperature that the cell can reach during the cycle is 289.5 K.

4.1.8 For single cell (cooled with 3M Novec 7100) under charge/discharge cycle:

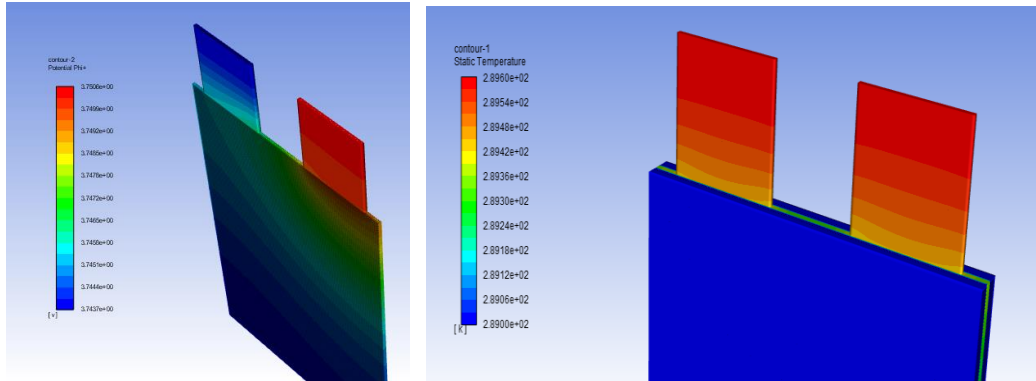


Figure 31 Contours for phi+ and static temperature of 3M novoc 7100 cooled cell under cycle

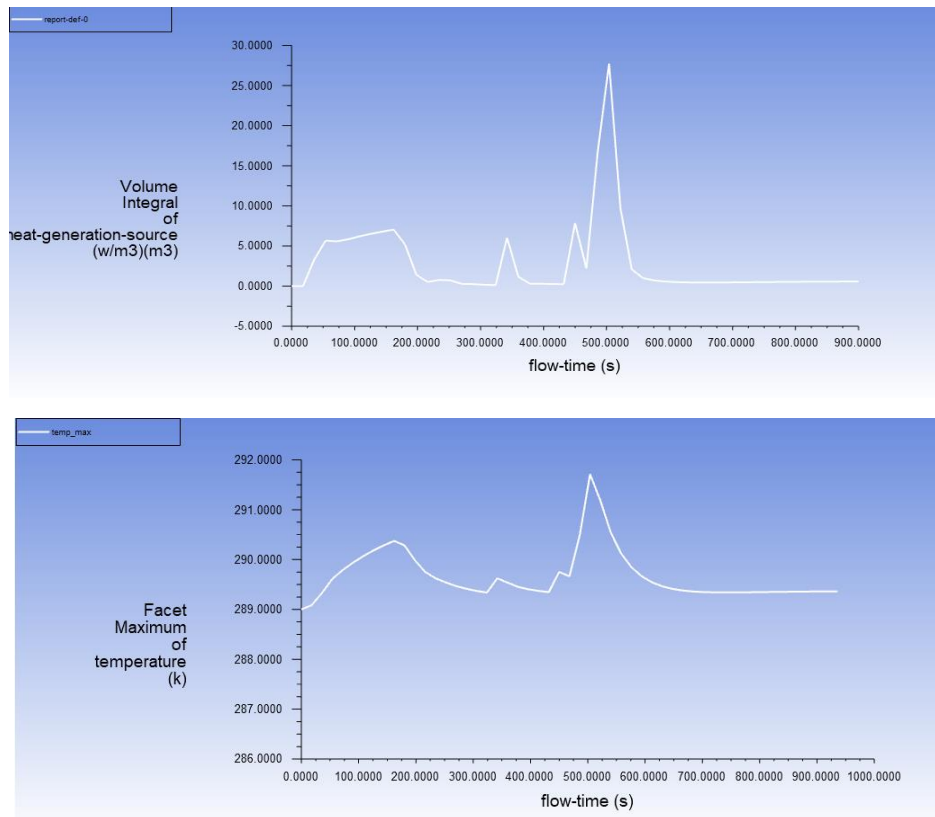


Figure 32 Plots for Total heat generation and Maximum temperature

From the figures shown above we can see that a 3M-Novec cooled cell with water flowing at 0.5 m/s sets the minimum temperature at 289 K and the maximum temperature that the cell can reach during the cycle is 291.6 K.

The results from the figures are summarized below:

Table 3 Maximum temperature variation for single cell cooled with various coolants

SN	Coolant	Max temperature	Min temperature
1	-	319.15 K	300 K
2	Air	298.41 K	289 K
3	Water	289.61 K	289 K
4	3M Novec 7100	291.6 K	289 K

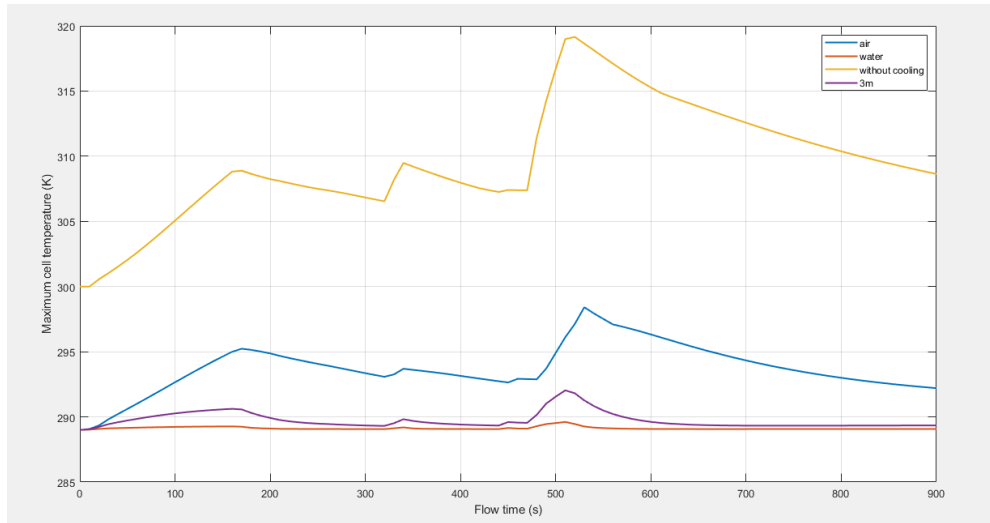


Figure 33 Maximum temperature across the charge discharge cycle with and without coolants

From this we can find that the cooling effect of water was better during the charge/discharge cycle. Also, the use of air water and 3M Novec 7100 brought the temperature of cell down by 6.49%, 9.26% and 8.49% respectively. And the use of these coolants set the minimum temperature of cell to 289 K.

4.2 For battery pack (LG Chem)

4.2.1 For battery pack under discharge:

4.2.1.1 Without coolant

At 0.3 C:

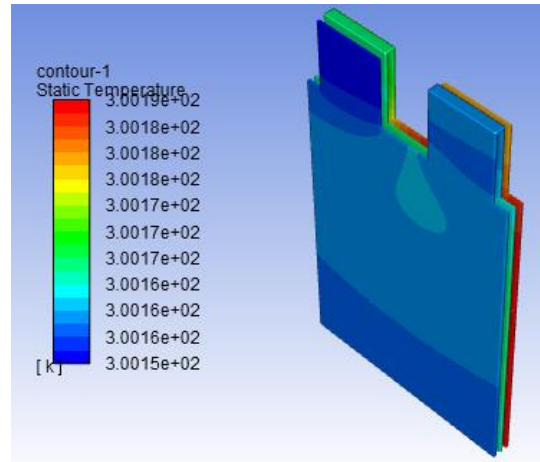


Figure 34 Temperature contour at 0.3 C

At 0.3 C discharge rate, the temperature of the battery pack increased minutely and the temperature change that occurred, occurred on the third cell that had the negative tab.

At 1 C:

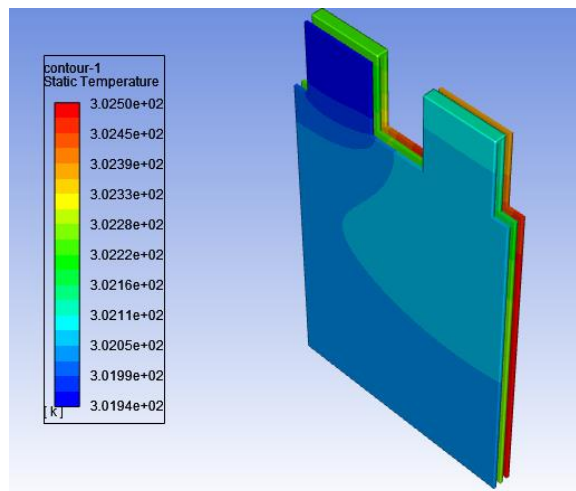


Figure 35 Plot for maximum temperature at 1C

At 1 C discharge rate, the temperature of the battery pack increases much more than that we observed with 0.3 C rate. The maximum temperature of the pack reaches to 302.5 K and the maximum temperature change occurred on the third cell that had the negative tab.

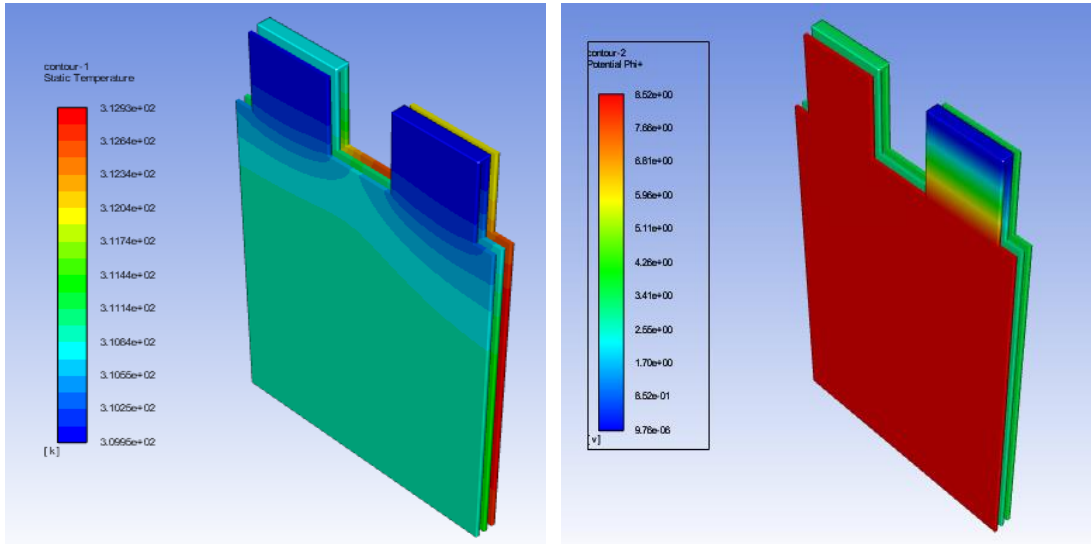


Figure 36 Temperature plot, Temperature and potential contours for 3C discharge rate of battery pack

At 3 C discharge rate, the temperature of the battery pack increases much more than that we observed with earlier C-rates. The maximum temperature of the pack reaches to 312.93 K and the maximum temperature change occurred on the third cell that had the negative tab. The minimum temperature of the cell was found to be 309.95 K.

From the above figures we can see that the temperature of a battery pack increases as the C rate increased.

4.2.1.2 For battery pack cooled with air under discharge:

At 0.3 c

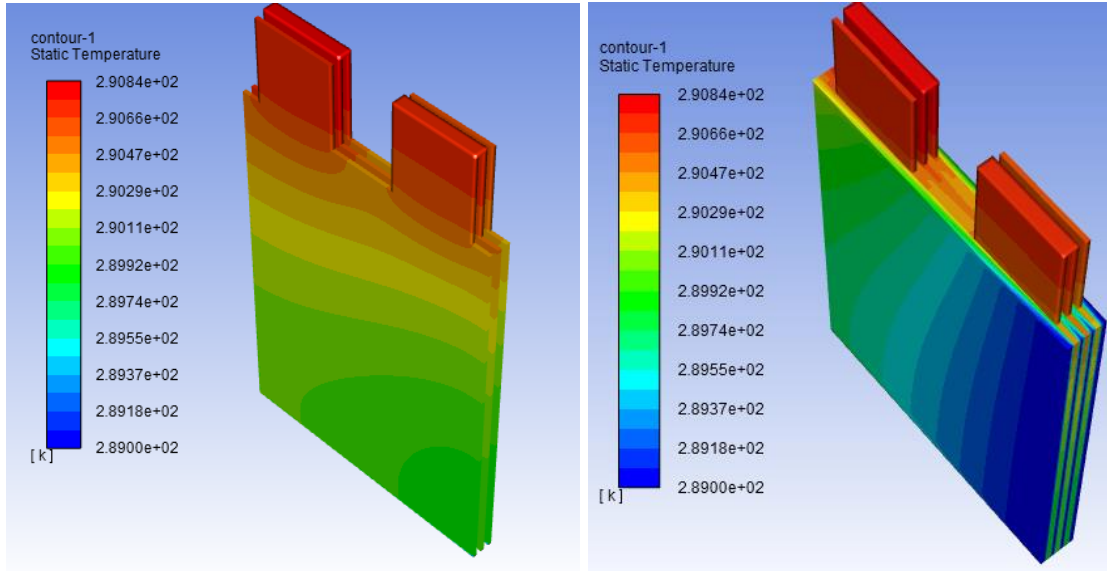


Figure 37 Temperature contour of the battery pack at 0.3 C rate

At 0.3 C discharge rate (flow time-1000s), the passive zones of the battery pack experience maximum temperatures. The maximum temperature of the pack reaches to 290.84 K. The minimum temperature of the cell was found to be 289 K. The area-weighted average potential of the battery pack was found to be 6.32 V.

At 1 C:

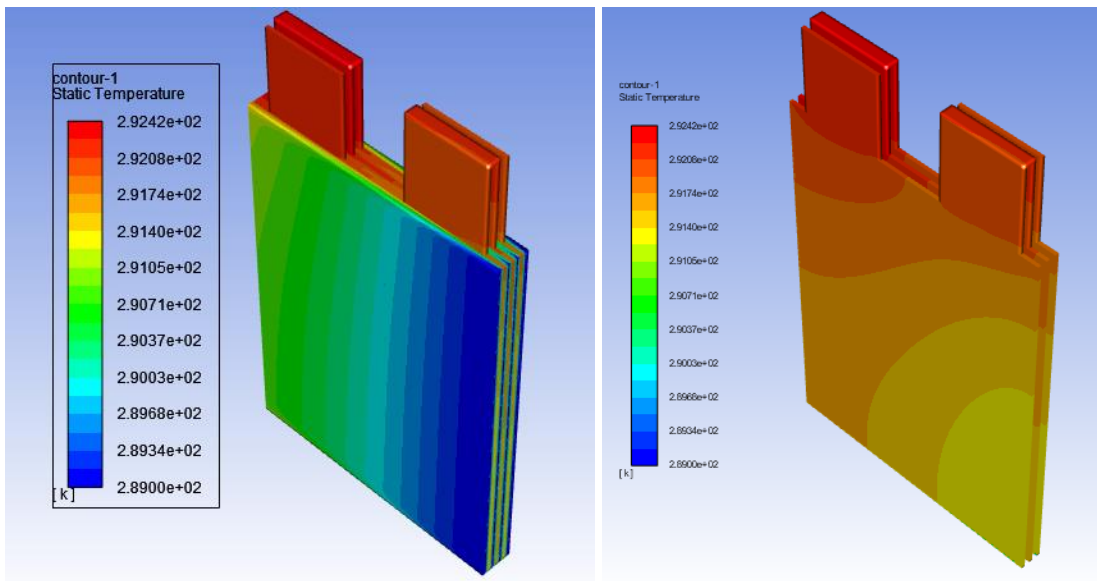


Figure 38 Maximum temperature and Temperature contour of battery pack at 1C

At 1 C discharge rate, the passive zones of the battery pack experience maximum temperatures. The maximum temperature of the pack reaches to 290.84 K. The cell zone of the battery also starts getting heated. The minimum temperature of the cell was found to be 289 K. The area-weighted average potential of the battery pack was found to be 5.13 V.

At 3 C:

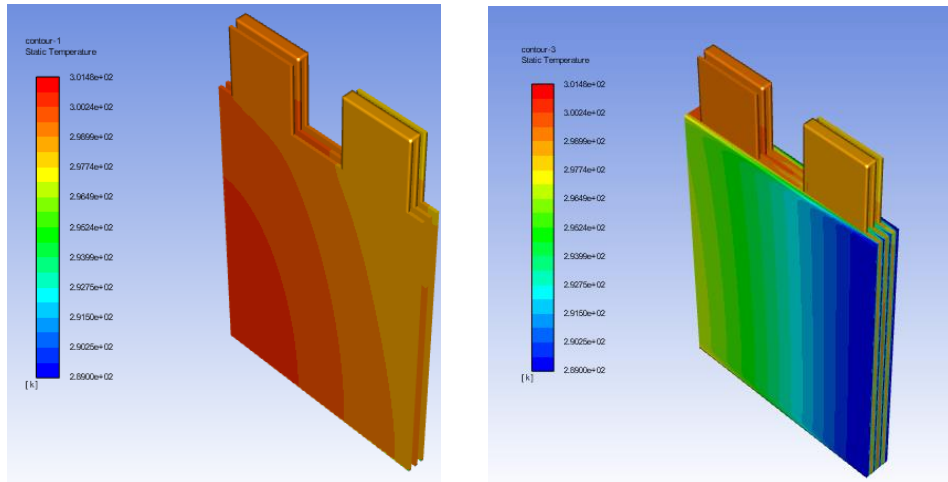


Figure 39 Maximum temperature and Temperature contour of battery pack at 3C

At 3 C discharge rate, the temperature of the battery pack increases much more than that we observed with earlier C-rates. The maximum temperature of the pack reaches to 301.48 K and the maximum temperature change occurred on the cell zones. The minimum temperature of the cell was found to be 289 K.

4.2.1.3 For water cooled battery pack :

At 0.3 C :

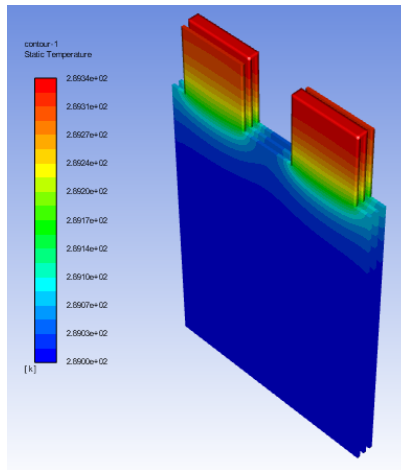


Figure 40 Temperature contour of water cooled system at 0.3 C

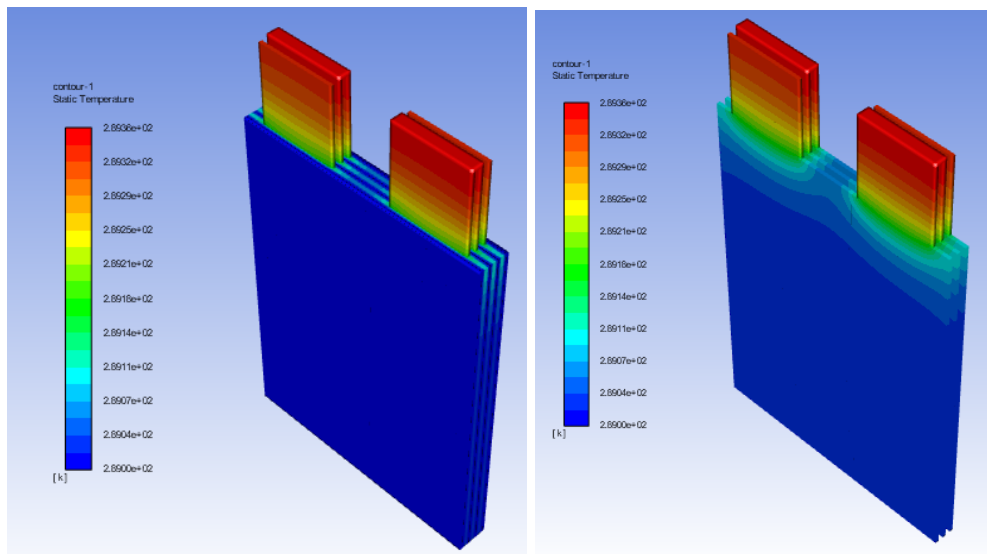


Figure 41 Temperature contour of water-cooled system at 1 C and 3C

In a water-cooled battery pack, the maximum temperature is 289.33947 K at the tabs and the minimum temperature is 289K. When the C-rate is raised to 1 C, the maximum temperature is 289.33947K at the tabs and the minimum temperature is 289K. Further when the battery is discharged at 3C the maximum temperature is 289.55244 K at the tabs and the minimum temperature is 289K.

4.2.1.4 For battery pack cooled with 3M Novec 7100 under discharge:

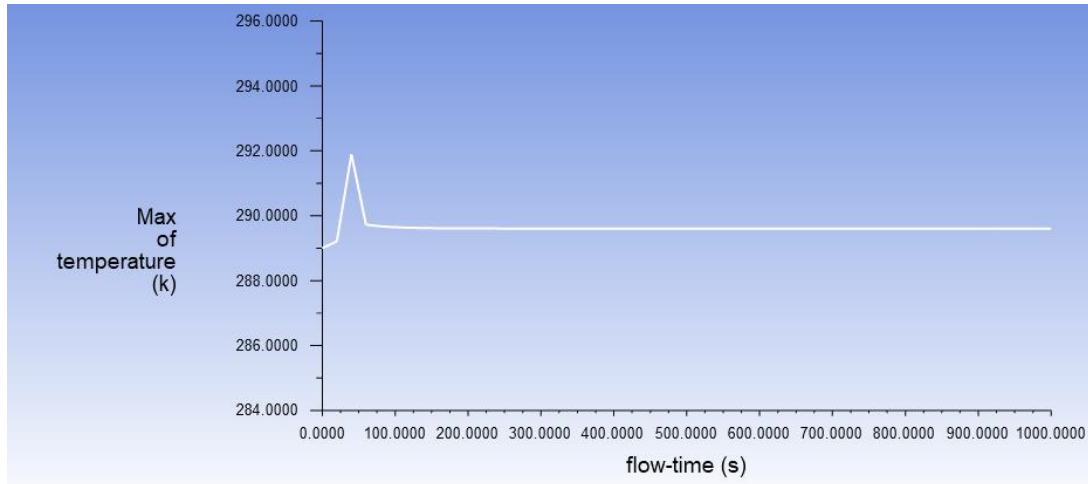


Figure 42 Maximum temperature of battery pack cooled by 3M Novec under discharge

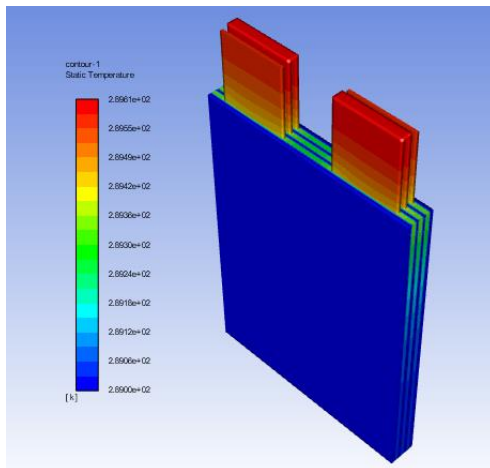


Figure 43 Temperature contour for 3-M Novec cooled pack at 0.3 C

At 0.3 C discharge rate, the temperature of the battery pack increases slightly. The maximum temperature of the pack reaches to 289.6 K and the maximum temperature change occurred on the passive zones (tabs and busbars). The minimum temperature of the cell was found to be 289 K.

With increase in C-rate to 1 C, the maximum temperature of the pack reaches to 289.76 K and the maximum temperature change occurred on the passive zones (tabs and busbars). The minimum temperature of the cell remained constant at 289 K.

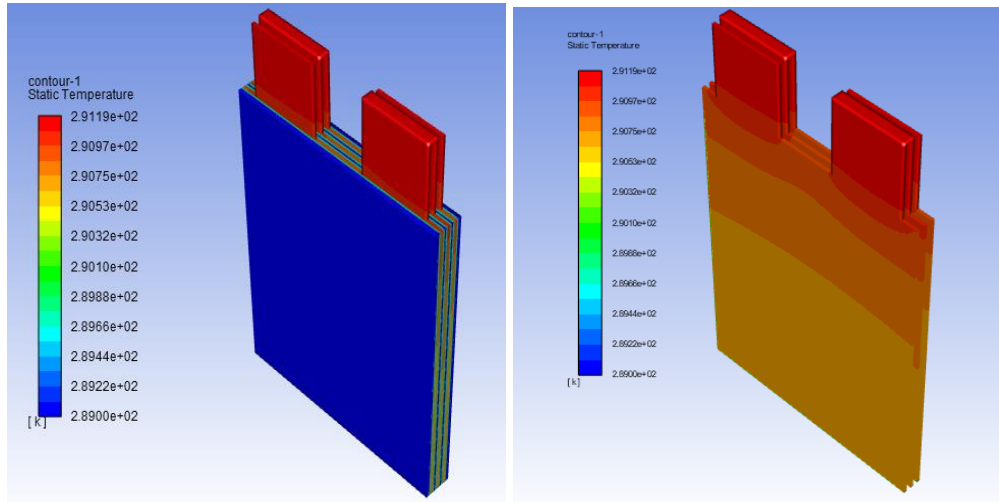
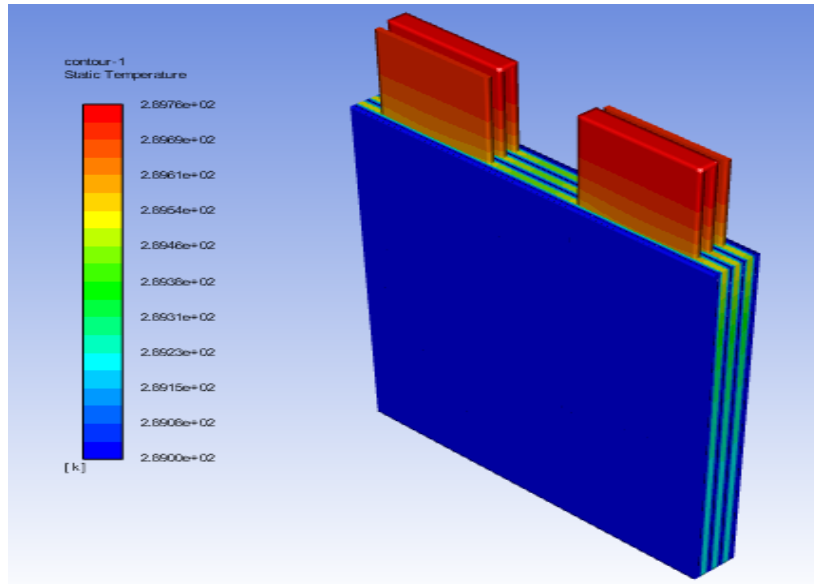


Figure 44 Temperature contour for 3-M Novec cooled pack at 1C and 3C respectively

At 3 C discharge rate, the temperature of the battery pack increases much more than that we observed with earlier C-rates. The maximum temperature of the pack reaches to 291.19 K and the maximum temperature change occurred on the tabs. The minimum temperature of the cell was found to be 289 K. The area weighted average potential of the battery pack was found to be 4.921907 V.

Table 4 Temperature variation for battery pack under different discharge cycle and coolants

SN	Coolant	Discharge rate	Max. Temperature	Min. Temperature
1	-	0.3	300.19 K	300K
	-	1	302.5 K	300K
	-	3	312.93	309.9K
2	Air	0.3	290.84236	289 K
	Air	1	292.42419	289 K
	Air	3	301.48 K	289
3	Water	0.3	289.33947 K	289K
	Water	1	289.35817	289K
	Water	3	297.81K	289K
4	3M Novec 7100	0.3	289.6 K	289K
	3M Novec 7100	1	289.76428 K	289K
	3M Novec 7100	3	291.1925	289K

From these figures and table, we can observe that the maximum temperature of the battery pack when discharged is less for case 4, so we can say that the cooling effect produced by 3M Novec 7100 is the best.

4.3 For battery pack running on charge/discharge cycle:

4.3.1 Without coolant

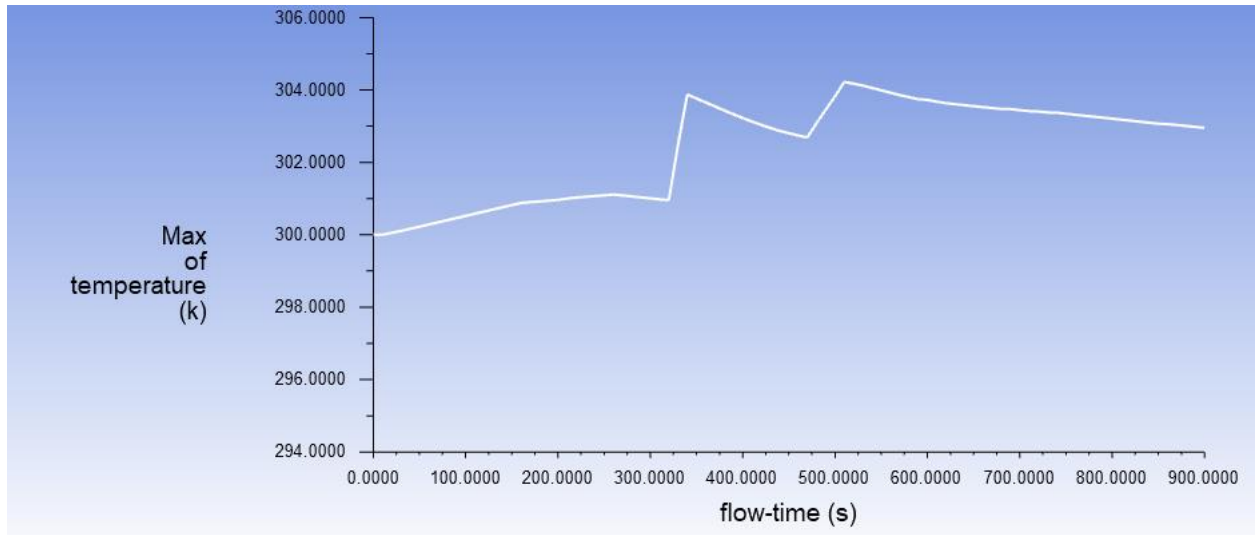


Figure 45 Variation of maximum temperature of pack across charge/discharge cycle

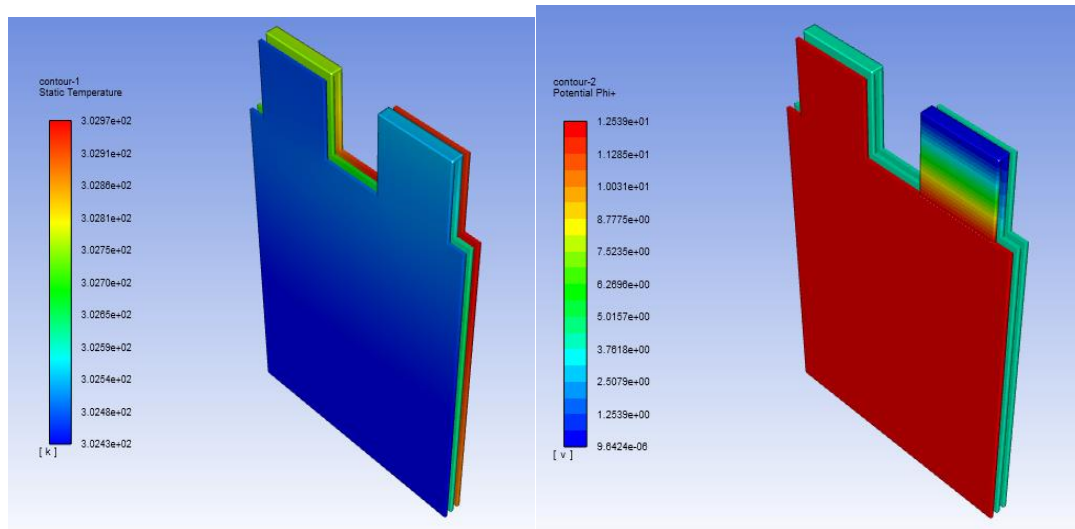


Figure 46 Temperature variation for battery pack under charge/discharge cycle

From figure 45, it can be found that the maximum temperature increase occurred during the charging of cell at 1 C for 400s, i.e., the 9th component of our cycle. The maximum temperature is found to be 304.2 K. The maximum temperature was observed in the cell

containing negative tab. It can also be seen that the potential of the battery decreases during the discharge processes and increases during the charging processes.

4.3.2 For air cooled battery pack under c/d cycle:

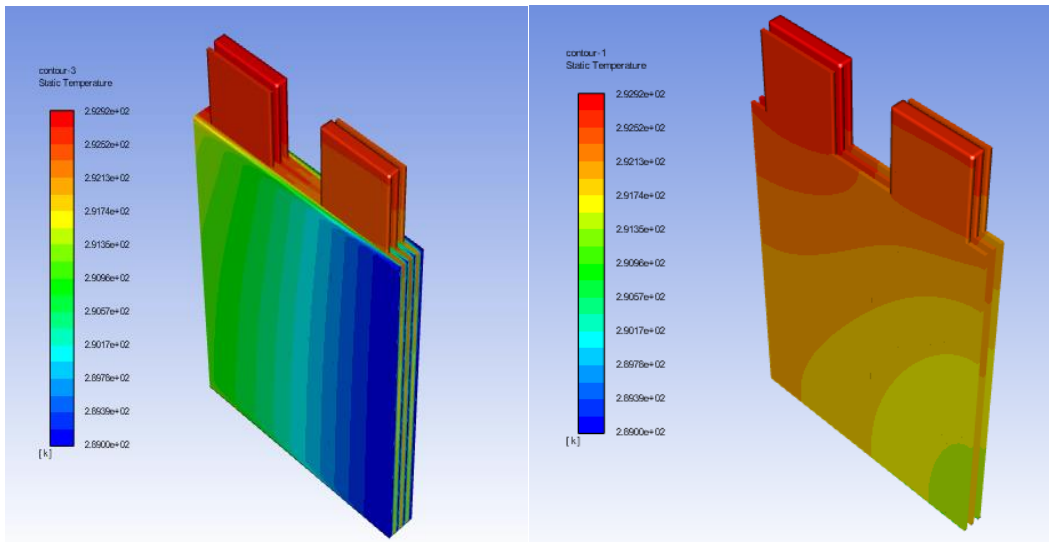
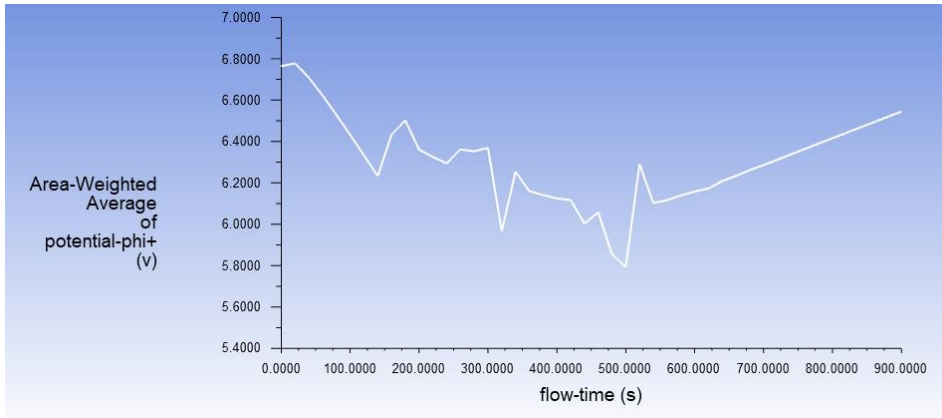
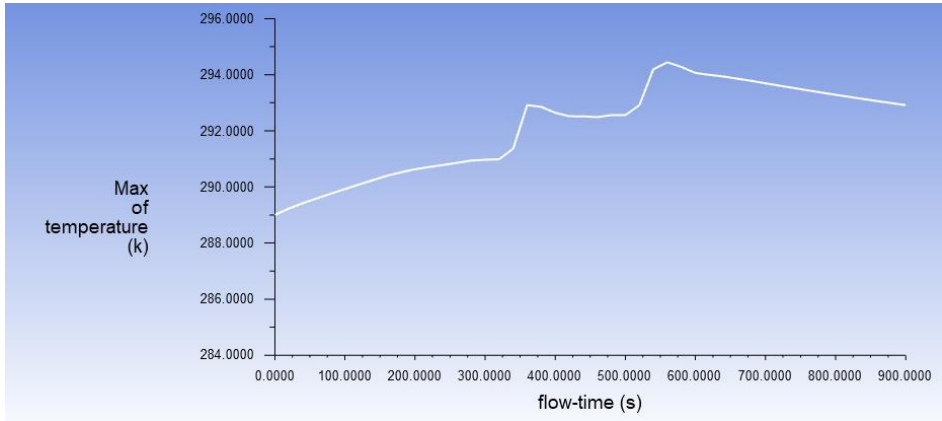


Figure 47 Plots for temperature, phi and temperature contour for air-cooled battery pack

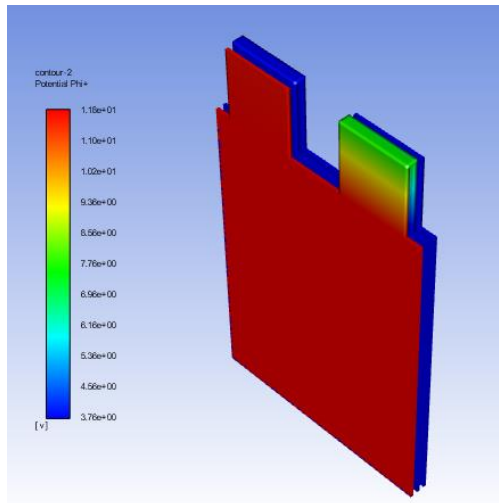


Figure 48 Potential contour of cell

By reviewing the plots, it can be found that the maximum temperature increase occurred during the discharge at 0.5 C for 100 s, i.e. the 6th component of our cycle. The maximum temperature is found to be 294.44 K. The maximum temperature was observed in the cell containing negative tab. It can also be seen that the potential of the battery decreases during the discharge processes and increases during the charging processes. The maximum positive potential is 11.8 V.

4.3.3 For water cooled battery pack under c/d cycle:

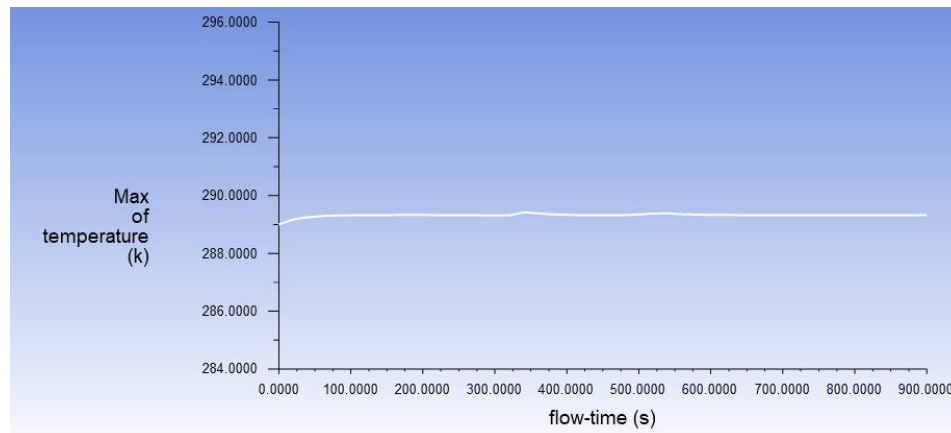


Figure 49 Maximum temperature across the drive cycle

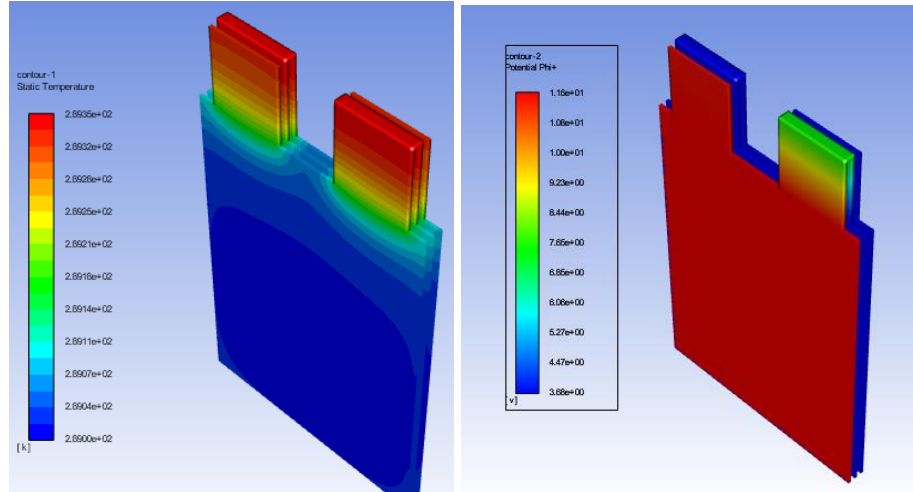
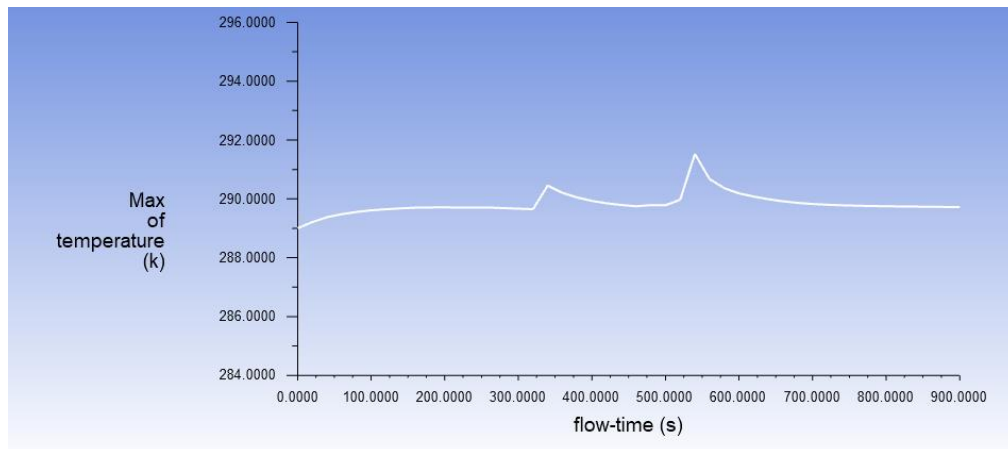


Figure 50 Temperature contour of water-cooled battery pack under c/d cycle

By figure 50, it can be found that the maximum temperature did not fluctuate a lot during this charge discharge cycle for the water-cooled battery. The maximum temperature is found to be 290.436 K. The maximum temperature was observed across the passive zones (i.e., the tabs and busbars).

4.3.4 For battery pack cooled by 3M Novec 7100 under c/d cycle:



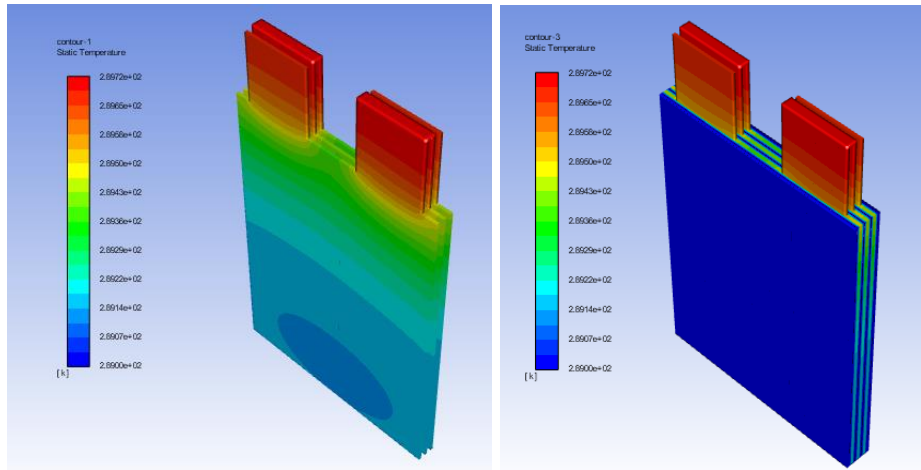


Figure 51 Maximum temperature plot and temperature contour for water cooled battery pack

By reviewing the plots in figure 51, it can be found that the maximum temperature did not fluctuate a lot during this charge discharge cycle for the water cooled battery. The maximum temperature is found to be 291.524 K. The maximum temperature was observed across the passive zones (i.e., the tabs and busbars).

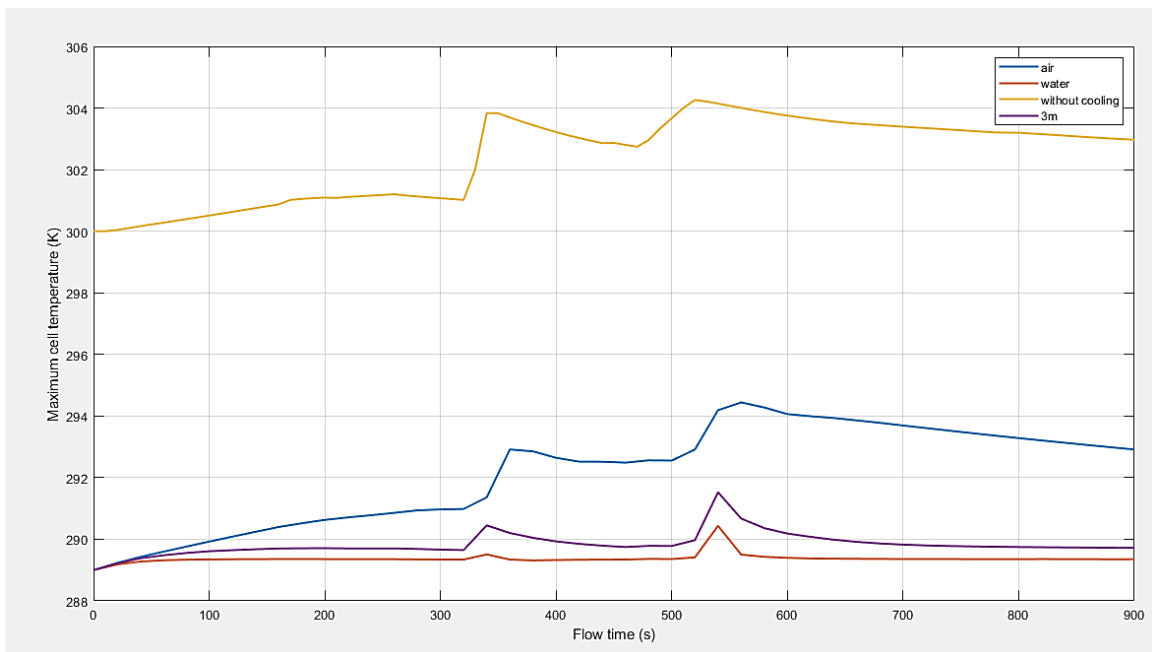


Figure 52 Maximum temperature vs flow time plots for battery pack with and without coolants

From figure 52 we can see that the peak temperature occurs between 500 to 600 s time intervals. The results were tabulated to show the maximum and minimum temperature for the four cases.

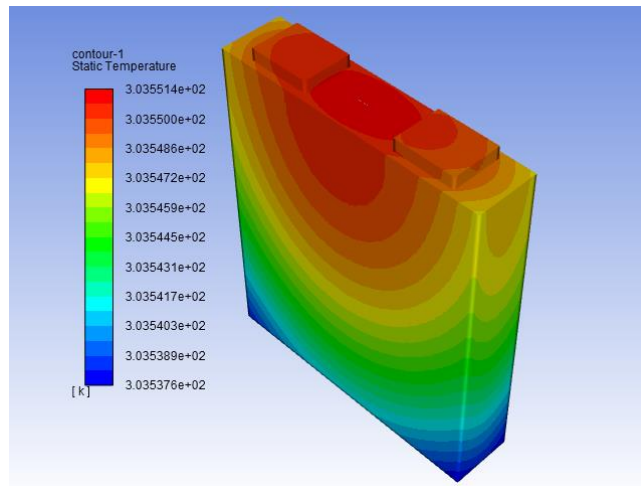
Table 5 Temperature variation for battery pack with and without coolants

SN	Coolant	Max temperature	Min temperature
1	-	304.26 K	302.43 K
2	Air	294.44 K	289 K
3	Water	290.436 K	289 K
4	3M Novec 7100	291.524 K	289 K

From the table it can be seen that Water can be used achieved the best cooling among the three coolants. Upon use of coolant on the cell, the temperature of the battery module lowers by 3.27%, 4.54% and 4.18 % for air cooled, water cooled and 3M Novec cooled battery module respectively. Hence, water shows better cooling properties among the other coolants.

4.4 For Highstar Cell :

4.4.1 For single cell under different discharge rates :



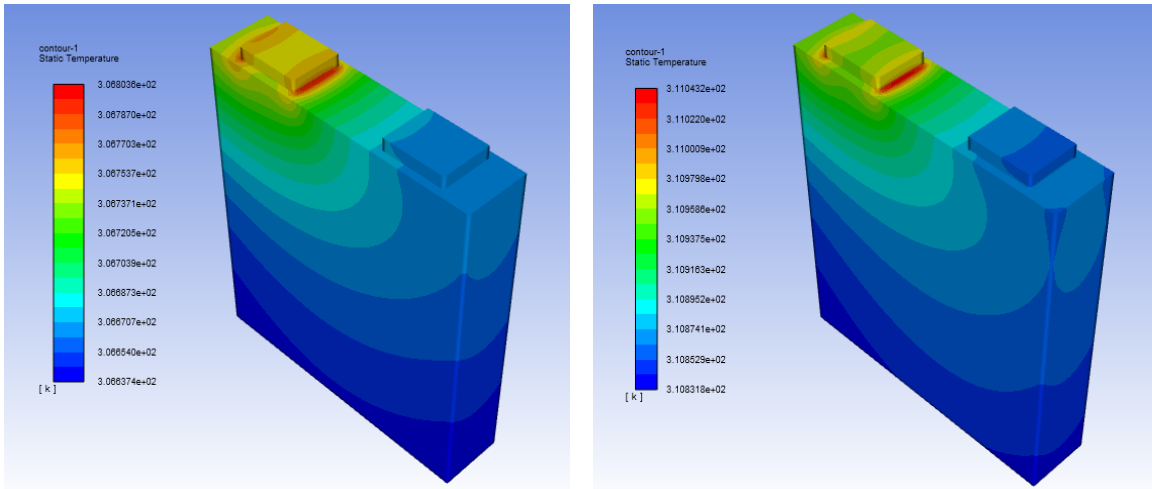
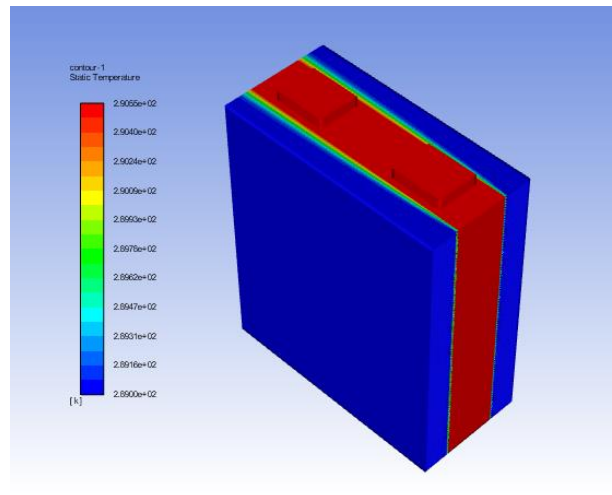


Figure 53 Temperature contour of cells at 0.3 C, 1C and 3C

It was seen that with increase in C rate the temperature of the cell increased drastically. The maximum temperature of 303.551 K, 306.8 K, 311.04 K was seen for cells when simulated with 0.3C, 1C and 3C rate respectively. Whereas for 3C, temperature reached maximum pretty soon. It can be seen that temperature homogeneity across the cell was affected by increasing the discharge rate.

4.4.2 For single cell (air cooled) under different discharge rates:



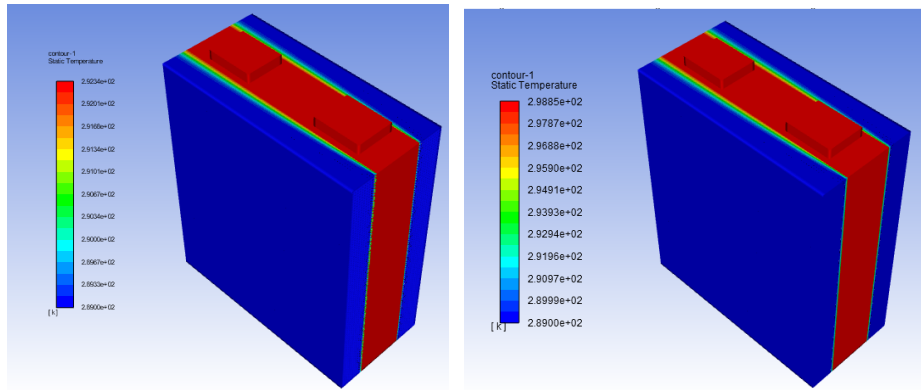


Figure 54 Temperature contour of air-cooled cells at 0.3, 1 and 3C

It was observed that the effect of increasing C rate on the cell increased the temperature. The maximum temperature of 290.55 K, 292.34K and 298.88K, K was seen for cells when simulated with 0.3C ,1C and 3 C rate respectively.

4.4.3 For Highstar cell cooled with Water:

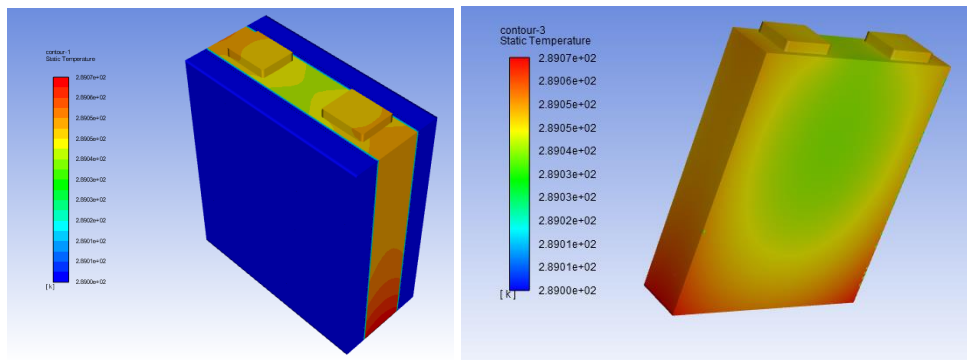


Figure 55 Temperature of cell with and without cooling fluid(water) at 0.3 C

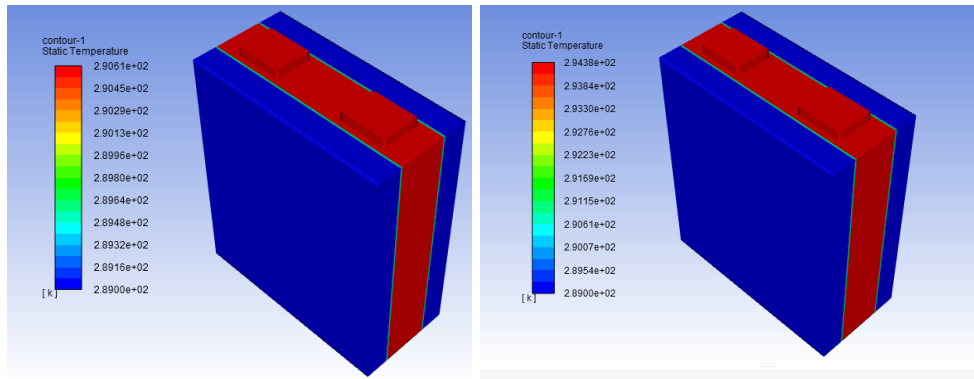
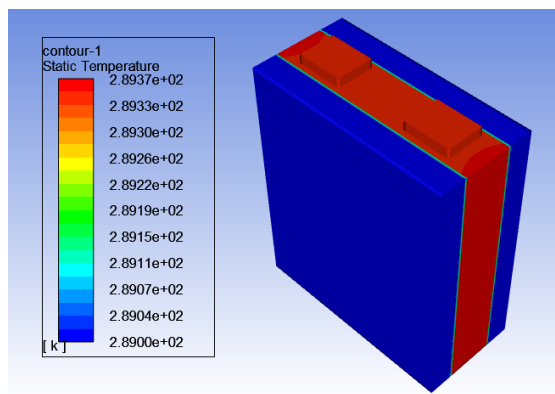


Figure 56 Temperature contour of cell cooled at 1C and 3C

When the cell is simulated at a c-rate of 0.3, we can see that the heat generated on the cell when it is cooled by a stream of water at 0.5m/s, 289K causes the temperature to rise to about 289.07K. As the discharge rate increases, maximum temperature of cell is seen to be 290.61 and 294.38K at 1C and 3C discharge rate respectively. The effect of cooling on the cell can be seen across the cooling channel. The minimum temperature that occurs across the surface is 289K.

4.4.4 For highstar cell cooled with 3m-Novec 7100:



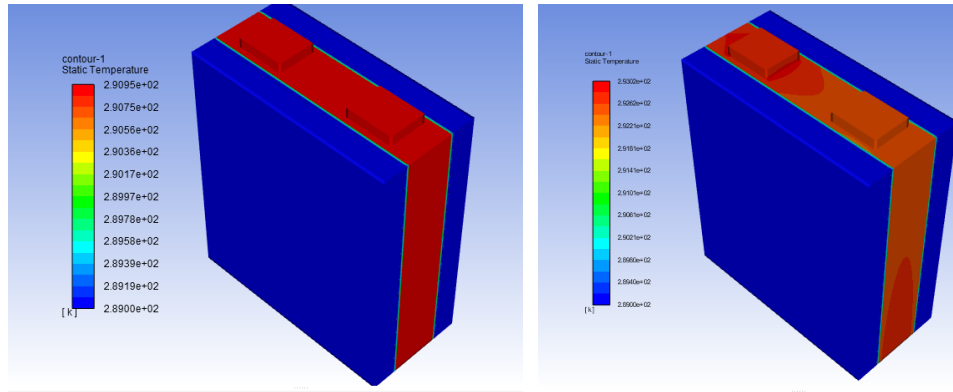


Figure 57 Temperature contours of cell cooled by 3M Novec 7100 at 0.3C, 1C and 3C

As seen earlier, with increase in C-rate the temperature contours show increase in the cell temperature. The maximum temperature of the cell increased from 289.37 K at 0.3 C to 293.03 K at 3C respectively.

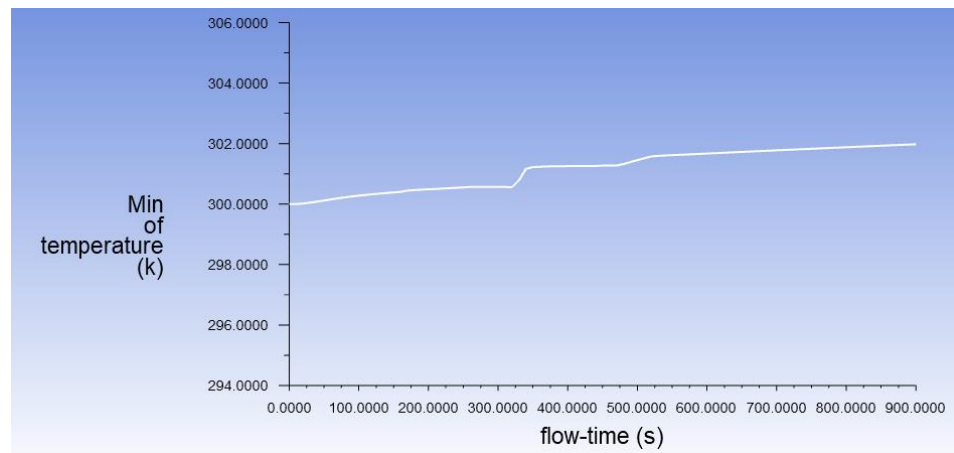
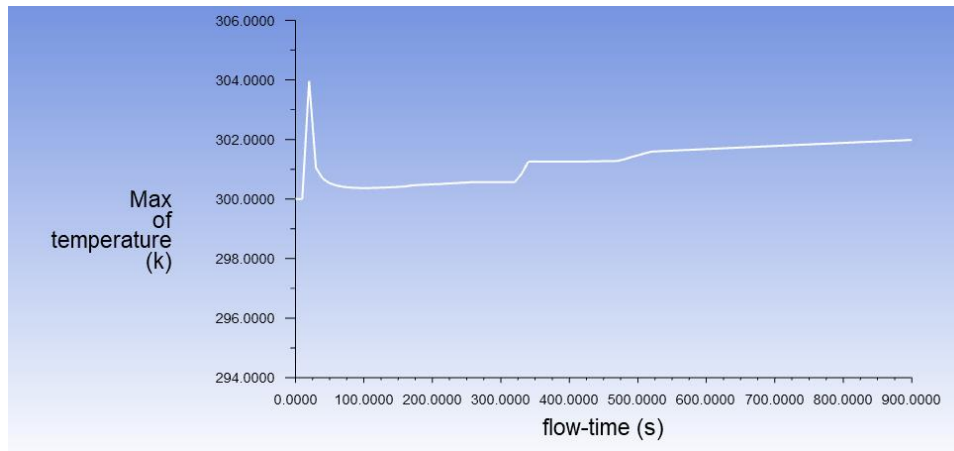
Table 6 Table for comparison of cooling for highstar cell

SN	Coolant	Discharge rate	Max. Temperature	Min. Temperature
1	-	0.3	303.35K	300K
	-	1	306.8K	300K
	-	3	311.04 K	300K
2	Air	0.3	290.55 K	289K
	Air	1	292.344 K	289K
	Air	3	298.88 K	289K
3	Water	0.3	289.07 K	289K
	Water	1	290.61K	289K
	Water	3	294.38 K	289K
4	3M Novec 7100	0.3	289.37K	289K
	3M Novec 7100	1	290.95 K	289K
	3M Novec 7100	3	293.03 K	289K

From these table, we can observe that the maximum temperature of the cell is least for when the cell is cooled by 3M Novec 7100. For lower discharge rates, the maximum temperature across the different cells is similar, but at higher discharge rates, 3M Novec 7100 produces appreciable cooling effect.

The simulation for this cell helps us understand that for a cell with different capacity (i.e 50Ah) the behavior shown by the cell is similar to that of LG Chem cell.

4.4.5 For single cell under charge/discharge curve:



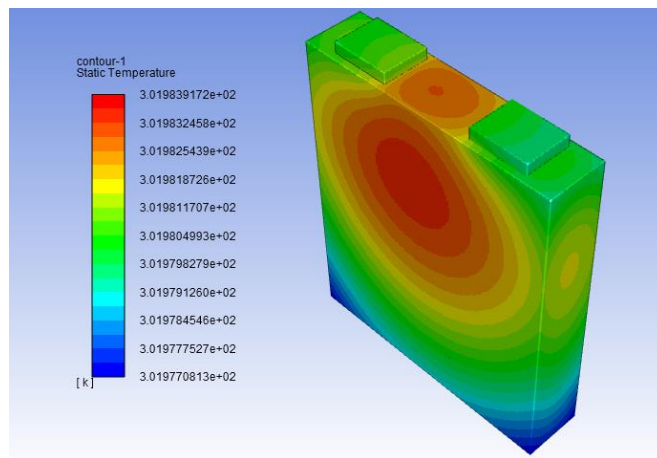
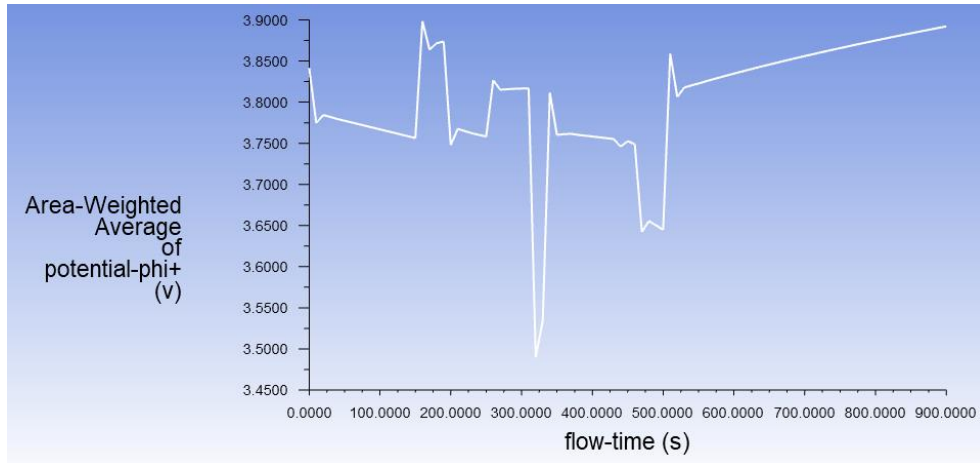


Figure 58 Temperature Contour, Maximum temperature, minimum temperature and positive potential plots

By reviewing the figure 59, it can be found that the maximum temperature increase occurred during the discharging of cell at 200W C for 150s, i.e. the 1st component of our cycle. The maximum temperature is found to be 303.9 K. It can also be seen that the potential of the battery decreases during the discharge processes and increases during the charging processes. But the volume of heat generation across the cell increases during discharge and decreases during charging processes.

4.4.6 For highstar cell using various coolants:

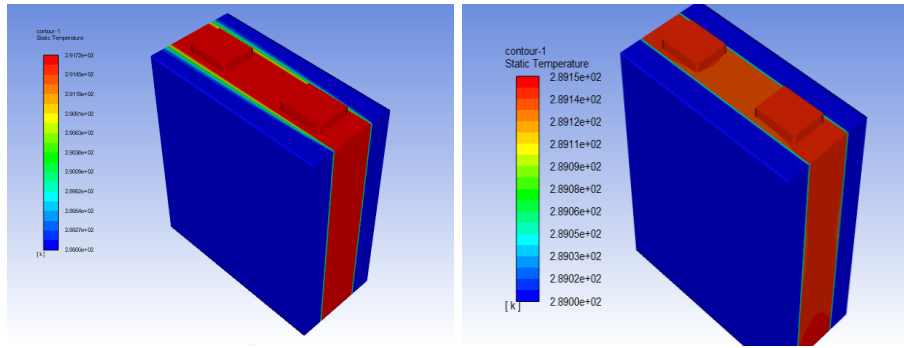


Figure 59 Temperature contour of cell cooled by air and water

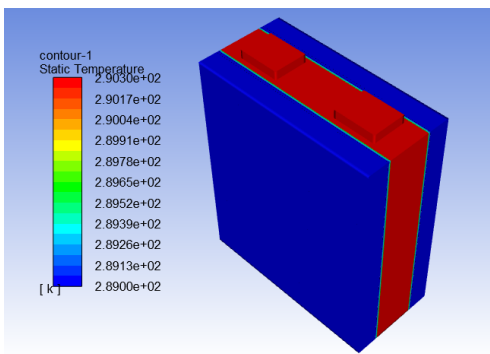


Figure 60 Temperature contour of cell cooled by 3M Novec 7100

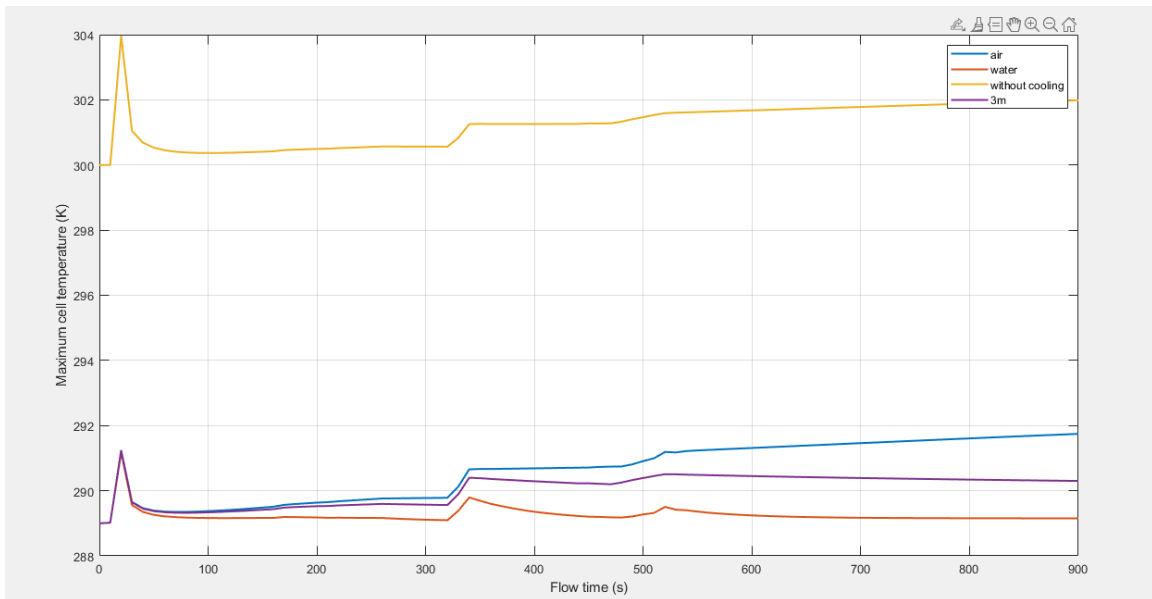


Figure 61 Comparison of temperature with and without coolants

Table 7 Temperature comparison for highstar cell under charge discharge cycle with different coolants

SN	Coolant	Max temperature	Min temperature
1	-	303.9651 K	300 K
2	Air	291.7459 K	289 K
3	Water	291.1782 K	289 K
4	3M Novec 7100	291.2359 K	289 K

From this we can find that the cooling effect of water was better during the charge/discharge cycle. Also, the use of air water and 3M Novec 7100 brought the temperature of cell down by 4.02%, 4.206% and 4.18% respectively.

4.5 Experimental Works:

The experimental setup consisted of electrical and electronic systems to charge, and perform discharge operations of the battery. The electrical and electronic system consisted of power switch, laptop (with EB tester software installed), electric connectors, a charger, an electric load (discharger), and several electrical connectors. An infrared contactless thermometer was used to measure the temperature of the battery during discharging applications.

The equipment used in this experiment were:

1. Thermometer
2. Charger
3. Discharger (Electronic Load)
4. Cell (lithium ion)

The module cell was charged to a 100% state of charge (SOC) before the start of the experiment.



Figure 62 Setup for conducting tests

4.5.1 Results:

A Highstar 3.2 V 50Ah battery cell was discharged at 0.3C discharge rate, and the measurement results were compared with the CFD thermal simulation of the cell at identical operating conditions. This testing was done at a temperature of 23 °C. The test value for current was 15A (0.3C).

The results obtained from the simulation can be presented in two different ways. The first result included the temperature of the battery as the discharge process was conducted. The next results that were obtained was the plot for voltage and current with time as the discharge process took place, which was obtained automatically from the EBtester software. For this result the input values were that of time, current to be released and cutoff voltage from the battery.

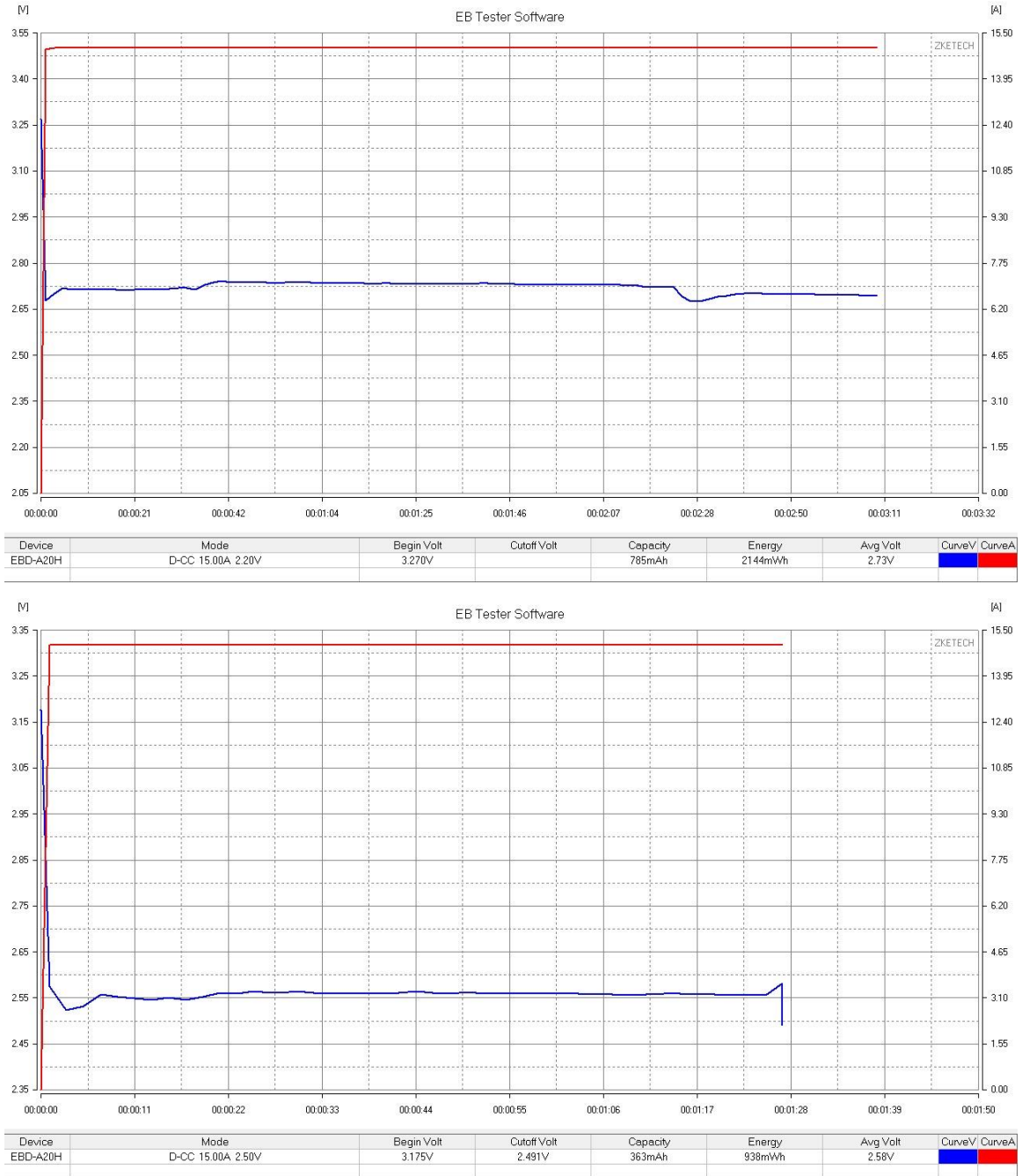


Figure 63 Voltage current plots for cell at 0.3C

From these plots the dip in positive potential (ϕ^+) can be easily observed in the discharging process. This was the plot obtained for the change in potential in 0.3 C discharge rate of the battery. This curve is similar to the one we found in ANSYS simulation.

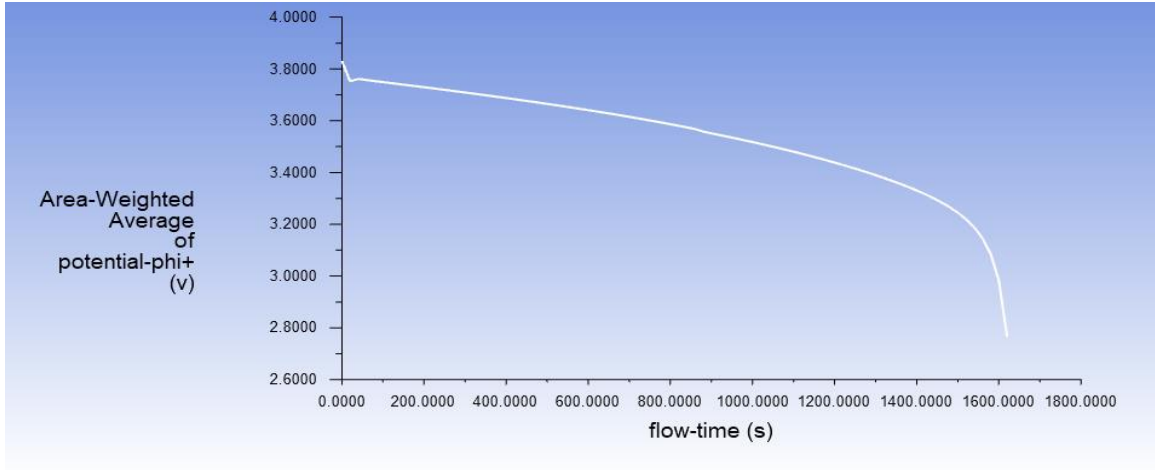


Figure 64 ϕ^+ plot from simulation at 0.3 C

The temperature of the cell on discharge was observed and the values at different time instances are given below:

Table 8 Temperature values obtained from tests

SN	Time(min)	Temperature
1	1	298
2	2	298.2
3	3	298.2
4	4	298.6
5	5	298.8
6	6	299.1
7	7	299.3
8	8	299.5
9	9	299.4
10	10	299.6

11	11	299.8
12	12	300.1
13	13	300.1
14	14	300
15	15	299.9

The values obtained from test at 23°C and from simulation in ANSYS were compared and it was found that the values were closely similar. The values obtained from simulation were in close agreement with the experimental values.

Also, the plot for temperature contour was obtained by simulation in ANSYS and is displayed in figure 67. The cell appears to be heated in the tabs and it is slowly transmitted across the center of the cell.

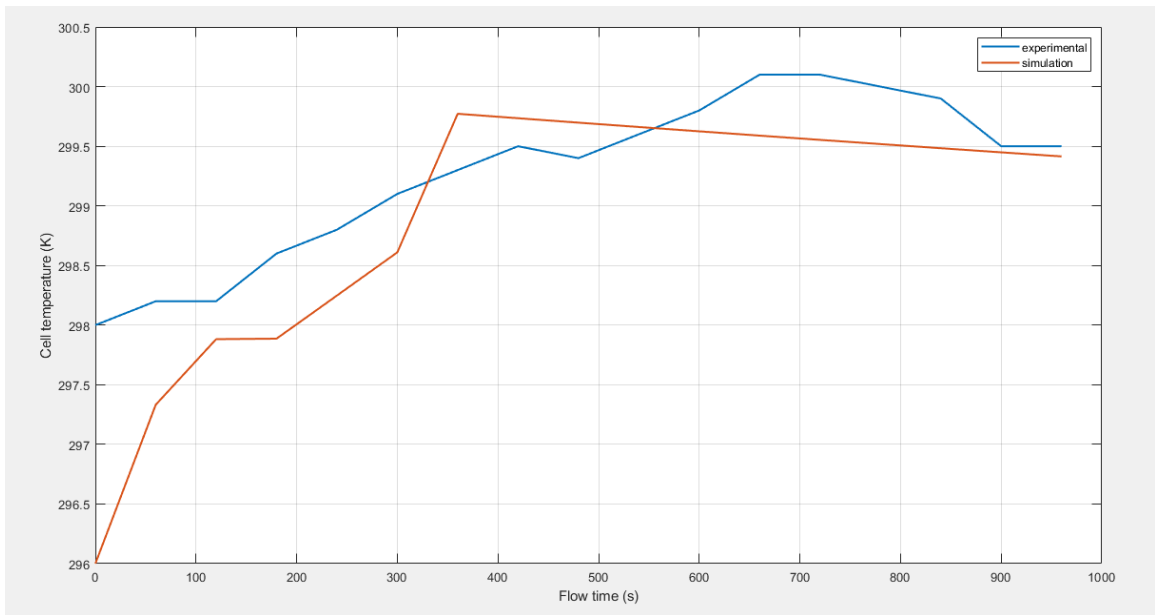


Figure 65 Experimental and simulation data for highstar cell at 0.3 C

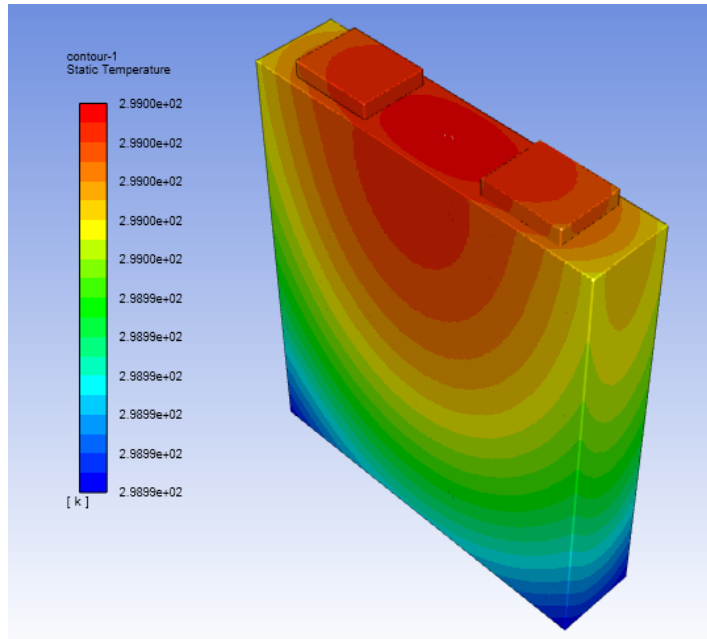


Figure 66 Temperature contour for simulation at 0.3C

CHAPTER FIVE: CONCLUSION AND RECOMMENDATIONS

5.1 Conclusion

So, upon completion of this thesis, temperature analysis of electric vehicle lithium-ion cell/ battery during discharging, and combined cycle was completed. This was done for two different cells in ANSYS. And to validate it, tests to observe the temperature increase in one of the cells (highstar) was performed.

It was found that on increasing the discharge rate, the maximum temperature of the cell increased. The effect of different coolants on the maximum temperature of the cell was observed and it was found that among the three different coolants used, 3M Novec-7100 proved to be the best coolant for simple discharge conditions.

Meanwhile when the cells were simulated according to combined cycle, water proved to be the best coolant for both the cells at 14.6 Ah and 50Ah.

5.2 Recommendations:

Following things can be recommended for further works in this field:

- Tests on cells at higher C-rates can be done to better analyze the temperature change
- Test to compare the cooling behavior can also be replicated in lab
- Since the temperature measurement was done with an infrared thermometer, there could be some flaws in it. So, use of IR cameras to obtain the temperature contour would be effective in temperature analysis of the cell
- Simulations to observe the temperature of the cell can also be done using MATLAB Simulink and OpenFOAM.
- Simulations to observe the behavior of the cell under drive cycle can be done using MATLAB Simulink and ANSYS

Appendix:



Figure 67 Experimental cell



Figure 68 Infrared contactless thermometer

Table 9 Experimental data and simulation

time	Simulation	experimental
0	296	298
60	297.3324	298.2
120	297.8822	298.2
180	297.8862	298.6
240	298.2479	298.8
300	298.6098	299.1
360	299.7721	299.3
420	299.7347	299.5
480	299.6977	299.4
540	299.6611	299.6
600	299.6248	299.8
660	299.5889	300.1
720	299.5533	300.1
780	299.5181	300
840	299.4833	299.9
900	299.4488	299.5
960	299.4146	299.5

REFERENCES

- Akturk, A., Yildiz, M., & Arıcı, M. E. (October 2021). Temperature Variation of a Li-Ion Battery Module Operated at the Driving Cycle for Different Cooling Rates. The 5th International Conference on Alternative Fuels, Energy&Environment (ICAFEE 2021): Future and Challenges.
- Amini, A., Özelci, B., & Tanılay Özdemir, e. a. (June 2020). Experimental Study of the Performance of a Li-Ion Battery Cell in a Highway Driving Cycle. *Kocaeli Journal of Science and Engineering*.
- ANSYS. (2015). ANSYS Fluent Battery Module Manual. ANSYS INC.
- Bharathwaaj, R., Mohanavel, V., Karthick, A., Vasanthaseelan, S., Ravichandran, M., Sakthi, T., & Rajkumar, S. (2022). Chapter 7.2 - Modeling of permanent magnet synchronous motor for zero-emission vehicles. In *Active Electrical Distribution Network*.
- Chen, M., & Rincon-Mora, G. A. (2006). Accurate Electrical Battery Model Capable of Predicting Runtime and I-V Performance. *IEEE Trans. On Energy Conversion*, 21.
- Conte, F. V. (2006). Battery and battery management for hybrid electric vehicles: a review. *Elektrotech. Inftech.* , 123, 424-431.
- Deng, D. (2015). Li-ion batteries: basics, progress, and challenges. *Energy Science and engineering*, 3(5), 385-418.
- Dhakal, R., Parameswaran, S., Muthukumar, R., & Moussa, H. (2022). Performance Analysis of Electrical Vehicle Battery Thermal Management System. SAE Technical Paper. doi:<https://doi.org/10.4271/2022-01-0204>
- evkx. (n.d.). Retrieved september 2023, from https://evkx.net/technology/battery/batterypack/?fbclid=IwAR3BNHIJS66YydGsPlxpgSSZQE4E4My_P27RB7HzxK2M2Yr3pxMb0oI_ixg
- Fayaz, H., Afzal, A., Samee, A. D., Soudagar, M. E., Akram, N., Mujtaba, M. A., . . . Saleel, Ü. A. (2022). Optimization of Thermal and Structural Design in Lithium-Ion Batteries to Obtain Energy Efficient Battery Thermal Management System (BTMS): A Critical Review. *Archives of Computational Methods in Engineering* volume, 29, 129-194.

- Holme, T. (n.d.). Quantumscape. Retrieved September 12, 2023, from <https://www.quantumscape.com/resources/blog/how-to-benchmark-solid-state-batteries/>
- Huber, C. K. (2015). Thermal management of batteries for electric vehicles. *Advances in Battery Technology for Electric Vehicles*, 327-358.
- Junchao Zhao, F. X. (2021). A comparative study on the thermal runaway inhibition of 18650 lithium-ion batteries by different fire extinguishing agents. *iScience*, 24(8).
- Kim, J., Oh, J., & Lee, H. (2019). Review on battery thermal management system for electric vehicles. *Applied Thermal Engineering*, 149, 192-212.
- Kwon, K. H., Shin, C. B., Kang, T. H., & Kim, C.-S. (2006). A two-dimensional modeling of a lithium-polymer battery. *Journal of Power Sources*, 163(1), 151-157.
- Liua, H., Weib, Z., He, W., & Zhao, J. (2017). Thermal issues about Li-ion batteries and recent progress in battery thermal management systems : A review. *Energy Conversion and Management*, 150, 304-330.
- Mansour Al Qubeissi, A. A.-A. (2022). Modelling of battery thermal management: A new concept of cooling using fuel. *Fuel*, 310.
- Michael.J. Lain, E. K. (2021). Understanding the limitations of lithium ion batteries at high rates. *Journal of Power resources*, 493.
- Motloch, C. G., Christophersen, J. P., Belt, J. R., Wright, R. B., Hunt, G. L., Sutula, R. A., . . . Miller, T. J. (2002). High-Power Battery Testing Procedures and Analytical Methodologies for HEV's. *SAE international*(0148-7191).
- Owen, R. E., Robinson, J. B., Weaving, J. S., & Pham, M. T. (2022). Operando Ultrasonic Monitoring of Lithium-Ion battery temperature and Behaviour at different cycling rates and under drive cycle conditions. *Journal of the Electrochemical Society*, 169.
- Panchal, S., Mathew, M., Fraser, R., & Fowler, M. (2018). Electrochemical thermal modeling and experimental measurements of 18650 cylindrical lithium-ion battery during discharge cycle for an EV. *Applied Thermal Engineering*, 135, 123-132.
- Pesaran A., G. S. (2013). Addressing the impact of temperature extremes on large format Li-ion batteries for vehicle applications. 30th int batter semin.

- Pesaran, A. A. (2002). Battery thermal models for hybrid vehicle simulations. *Journal of Power Sources*, 110(2), 377-382.
- Qasmi, Z. u., Afzal, D. M., Nadeem, M. T., Hossain, M. K., & al., e. (October 2022). ANSYS simulation of Temperature of Cooling System in Li-ion Battery. 8th International Exchange and Innovation Conference on Engineering & Sciences (IEICES), 8. Fukuoka, Japan.
- Reis, G. d., Strange, C., Yadav, M., & Li, S. (2021). Lithium-ion battery data and where to find it. *Energy and AI*, 5.
- Sun, J., Li, J., Zhou, T., Yang, K., Wei, S., Tang, N., . . . Chen, L. (2016). Toxicity, a serious concern of thermal runaway from commercial Li-ion battery. *Nano Energy*, 27, 313-319.
- Teng, H. (2012). Thermal Analysis of a High-Power Lithium-Ion Battery System with Indirect Air Cooling. *SAE International*, 79-88.
- Ui Seong Kim, a. J. (2011). Modeling the Dependence of the Discharge Behavior of a Lithium-Ion Battery on the Environmental Temperature. *Journal of The Electrochemical Society*.
- Vikram, S., Vashisht, S., & Rakshit, D. (November 2022). Performance analysis of liquid-based battery thermal management system for Electric Vehicles during discharge under drive cycles. *Journal of Energy storage*, 55.
- Vyroubal, P., Kazda, T., Maxa, J., & Vondrák, J. (2015, December). Analysis of Temperature Field in Lithium Ion Battery by Discharging. *ECS Transactions*.
- Yang, Z., Patil, D., & Fahimi, B. (Jan. 2019). Electrothermal Modeling of Lithium-Ion Batteries for Electric Vehicles. *IEEE Transactions on Vehicular Technology*, 68(1), 170-179.

Temperature analysis of Lithium Ion cell

ORIGINALITY REPORT

18%

SIMILARITY INDEX

PRIMARY SOURCES

1	www.researchgate.net Internet	231 words — 2%
2	evkx.net Internet	192 words — 2%
3	www.open-access.bcu.ac.uk Internet	143 words — 1%
4	www.e3s-conferences.org Internet	104 words — 1%
5	www.mdpi.com Internet	90 words — 1%
6	Aikun Tang, Jianming Li, Liusheng Lou, Chunxian Shan, Xuezhen Yuan. "Optimization design and numerical study on water cooling structure for power lithium battery pack", Applied Thermal Engineering, 2019 Crossref	55 words — < 1%
7	iopscience.iop.org Internet	52 words — < 1%
8	Shuwen Zhou, Yuemin Zhao, Shangyuan Gao. "Analysis of Heat Dissipation and Preheating Module for Vehicle Lithium Iron Phosphate Battery", Energies, 2021	46 words — < 1%